mRNA and drug delivery with lipid-based nanoparticles

Zeng, Y.

Citation

Zeng, Y. (2022, December 6). *mRNA and drug delivery with lipid-based nanoparticles*. Retrieved from https://hdl.handle.net/1887/3492640

Version:	Publisher's Version
License:	Licence agreement concerning inclusion of doctoral thesis in the Institutional Repository of the University of Leiden
Downloaded from:	https://hdl.handle.net/1887/3492640

Note: To cite this publication please use the final published version (if applicable).

Chapter 2

Efficient mRNA Delivery Using Fusogenic Coiled-coil Peptides

Abstract

Gene delivery has great potential in modulating protein expression in specific cells to treat diseases. Such therapeutic gene delivery demands sufficient cellular internalization and endosomal escape. Of the various nonviral nucleic acid delivery systems, lipid nanoparticles (LNPs) are the most advanced. Unfortunately most nonviral delivery systems like LNPs, are very inefficient in delivering nucleic acids to cells as the large majority is unable to escape endosomes/lysosomes. Here, we develop a highly efficient gene delivery system using fusogenic coiled-coil peptides. We modified LNPs, carrying EGFP-mRNA, and cells with complementary coiled-coil lipopeptides. Coiled-coil formation between these lipopeptides induced fast nucleic acid uptake and enhanced GFP expression. The cellular uptake of coiled-coil modified LNPs is likely driven by membrane fusion thereby omitting typical endocytosis pathways. This direct cytosolic delivery circumvents the problems commonly observed with the limited endosomal escape of mRNA. Therefore fusogenic coiled-coil peptide modification of existing LNP formulations to enhance nucleic acid delivery efficiency could be beneficial for several gene therapy applications.

Introduction

An understanding of both the human genome and disease mechanisms has expanded our knowledge of gene-dysregulation related diseases, paving the way for novel gene therapies.[1-3] Gene therapy potentially enables the treatment of disease at the genetic level by correcting or replacing malfunctioning genes.[4] This repair or replacement could be achieved by delivering exogenous nucleic acids such as DNA, mRNA, small interfering RNA (siRNA), microRNA (miRNA), or antisense oligonucleotides (ASO) to the tissue or organ of interest.[2] However, the complexity of cell membranes and cellular barriers impedes the efficient transfer of the genetic cargo into the organs, tissue, and cells of interest, resulting in a poor therapeutic effect.[4,5]

Since nucleic acid-based drugs are unable to enter cells and are inherently unstable *in vivo*, a drug delivery system is required. An ideal gene vector should transfect the desired tissue or organ efficiently, while the vector should be non-toxic, non-immunogenic, and ideally easy to formulate. State-of-the-art gene vectors are divided into two major classes: viral and nonviral. As viral vectors typically possess high cellular transduction efficiency, many gene therapy clinical trials are using modified viral vectors such as lentiviruses, retroviruses, adenoviruses, and adenovirus-associated viruses.[4,6-8] However, widespread use of viral vectors is hampered because of side-effects including potential carcinogenesis, immunogenicity, broad tropism, limited DNA packaging capacity, and difficulty of vector production.[2,9,10] In contrast, nonviral vectors could potentially circumvent these limitations, especially in terms of safety and the size of encapsulated genetic cargo.[11] Nonviral gene vectors in (pre)clinical applications are commonly composed of lipids,[12] lipoids,[13] or are polymer-based.[2]

Currently, the most advanced nonviral nucleic acid delivery system is lipid nanoparticles (LNPs).[14,15] LNPs are composed of an ionizable lipid to condense the genetic cargo and release it after entering the cells; a cholesterol moiety to stabilize the LNP structure; a helper lipid; and a PEGylated lipid to improve colloidal stability and reduce protein absorption.[16] The first siRNA drug, named Onpattro (Patisiran), was approved in 2018 by the FDA and was designed to treat polyneuropathies induced by hereditary transthyretin-mediated amyloidosis (hATTR) in adults. This therapy has been a milestone for nonviral nucleic acid-based therapies.[1] Onpattro is a lipid nanoparticle (LNP) formulation that upon intravenous administration binds serum apolipoprotein E (ApoE), which acts as an endogenous targeting ligand to the low-density lipoprotein receptor present in hepatocytes.[17]

LNPs cell entry relies on endocytosis, and the efficacy is dependent on the delivery of encapsulated siRNA to the cytoplasm.[15] However, LNPs (and other nanoparticles) transport the encapsulated macromolecules to different subcellular destinations, the majority of which accumulates in lysosomes for degradation.[18] Studies showed only <2% of the siRNA in LNPs was able to escape endosomal compartments, resulting in release into the cytoplasm;[19] and <5% of cytoplasmic mRNA of LNPs was distributed outside of endosomes, corresponding to endosome escaped events.[20] Therefore, there is an urgent need to overcome this major limitation of inefficient nucleic acid delivery into cells. Many attempts have been reported to facilitate endosomal escape by using polyplex-mediated endosomal swelling nanomaterials,[21,22] cell-penetrating peptides (CPPs),[23,24] or exogenous stimuli-responsive biomaterials responding to specific biochemical conditions, such as a change in pH or redox state but to date, there is still a lack of modified systems resulting in efficient endosomal

escape.[21,25]

One way that cells transfer components is via membrane fusion. Therefore, membrane fusion is critical for many biological processes, including organelle inheritance in cell growth and division, chemical synaptic transmission in the nervous system, and the modulation of synaptic strength in memory and learning.[26] The docking of transport vesicles to the target plasma membrane in neuronal exocytosis is triggered by coiled-coil formation between complementary SNARE protein subunits.[27] Inspired by the SNARE protein complex, our group has developed a synthetic membrane fusion system based on a heterodimeric coiled-coil peptide pair and we have demonstrated direct drug delivery into the cytosol of living cells *in vitro* and *in vivo*.[28-30]

In this study, we applied our fusogenic coiled-coil peptides to efficiently deliver LNPs into cells to enhance genetic cargo transfection efficacy via membrane fusion. We developed coiled-coil peptide modified LNPs encapsulating EGFP-mRNA to induce efficient cellular delivery and concomitant GFP expression (**Scheme 1**). The Onpattro LNP formulation was modified with lipopeptide CPE4 (CPE4-LNP) while cells were pretreated with the complementary lipopeptide CPK4. The addition of CPE4-LNP to the cells resulted in efficient LNP uptake and protein expression, which was observed and studied by confocal microscopy and flow cytometry. By applying different endocytosis inhibitors and a lysosome tracker, the internalization pathway was investigated. This study demonstrates that, by utilizing coiled-coil peptides, significant amounts of genetic cargo can be delivered to cells by evading endocytosis pathways.

Results

Comparison of K3/E3 and K4/E4 coiled-coil interactions

Our previous studies showed that both the K3/E3 and K4/E4 coiled-coil pairs (where 3 and 4 correspond to the number of heptad repeats within the peptides), induced efficient and targeted membrane fusion between liposomes, and liposomes with cells, both *in vitro* and *in vivo*.[28-30] In order to determine which pair was most suitable for this study we evaluated their coiled-coil forming and cargo delivery properties. Circular dichroism (CD) spectroscopy (**SI Fig. 1a**), confirmed both K3/E3 and K4/E4 pairs formed coiled coils efficiently. The K4/E4 pair is composed of one additional heptad repeat compared to K3/E3, and as expected the former peptide pair yielded a more-folded complex. Cellular internalization of En-modified fluorescent liposomes in Kn-modified HeLa cells was subsequently quantified by flow cytometry (**SI Fig. 1b**), demonstrating that both K3/E3 and K4/E4 induced cellular uptake, however K4/E4 exhibited significantly higher cell uptake. When comparing the mean fluorescence intensity (MFI) of fluorescent cells (**SI Fig. 1c-1d**), we observed that the K4/E4 pair is the most fusogenic as the cells showed the highest levels of fluorescence. We also observed that CPK4 modified liposomes were able to enter cells efficiently, even in the absence of E4 on the cell surface, presumably dues to interactions between the positively charged CPK4 lipopeptides and the negatively charged cell membranes.

Next, we studied whether these findings were also valid for the delivery of LNPs to cells. We formulated LNPs encapsulating Alexa488-labeled nucleic acid and modified these with 1 mol% of either CPE3 or CPE4 yielding CPE3-LNP and CPE4-LNP. HeLa cells were pretreated with the complementary CPKn and internalization of the LNPs was quantified by fluorescence measurements.

Again, the CPK4/CPE4 pair exhibited enhanced cellular internalization as compared to the CPK3/CPE3 pair (**SI Fig. 1e-1f**).

Therefore, we utilized the K4/E4 peptide pair with CPK4 at the cell membrane and CPE4 in the LNPs in the following experiments to achieve optimal coiled-coil formation and to exclude undesirable electrostatic interactions between positive CPK4 decorated LNPs and negatively charged cell membrane.

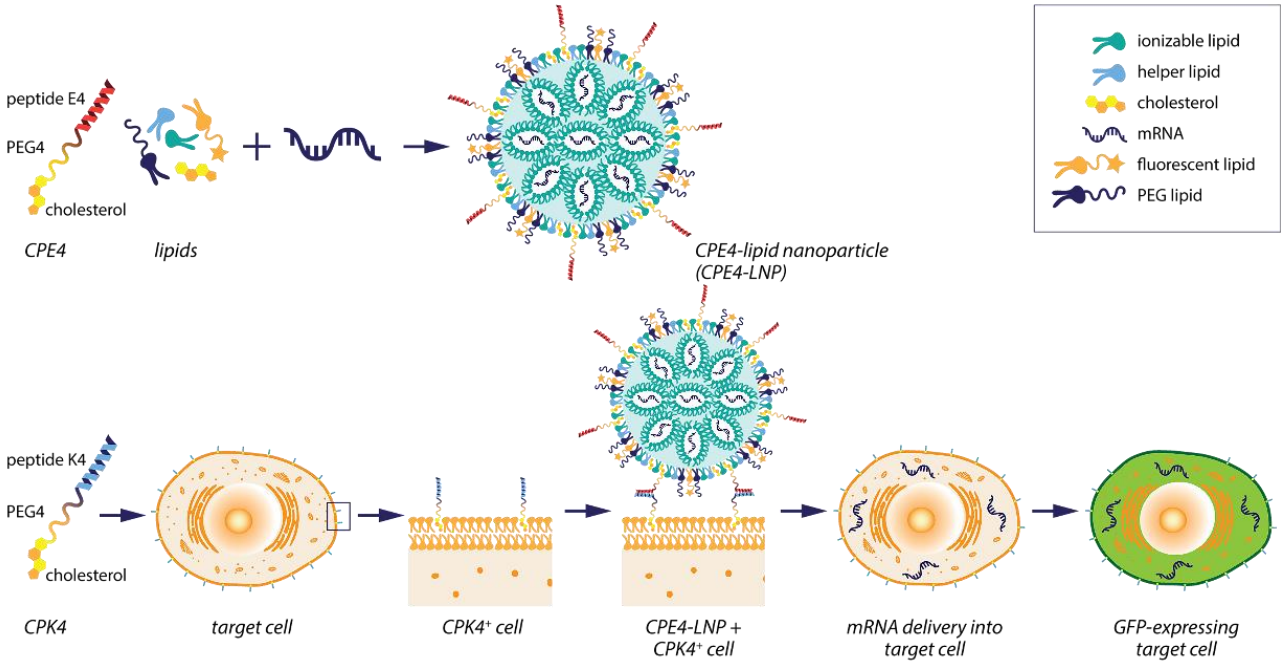

Scheme 1. *Schematic representation of the nonviral lipid nanoparticles (LNPs) that induce efficient mRNA delivery within cells when modified with fusogenic coiled-coil peptides.*

Lipid nanoparticle characterization

The lipid composition of the clinically approved LNP formulation Onpattro (Dlin-MC3-DMA:cholesterol:DSPC:DMG-PEG2K=50:38.5:10:1.5) has been optimized for potent silencing of protein expression in cells by delivery of siRNA.[1] To investigate the efficacy of coiled-coil mediated mRNA delivery into cells, we opted to formulate CPE4-LNPs with the same lipid composition as Onpattro and added 1 mol% of CPE4 (**Fig. 1a-b**). Dynamic light scattering (DLS) was used to determine the hydrodynamic diameters of both plain and CPE4-modified LNPs after encapsulating EGFP-mRNA. These diameters were found to be 80 and 95 nm respectively with low polydispersities (PDI) (**Fig. 1c**). Both formulations had a near-neutral zeta-potential, thus the presence of 1 mol% CPE4 did not influence the surface charge significantly. mRNA encapsulation efficiency was slightly lower for CPE4-LNP, which might be due to electrostatic repulsion between the negatively charged peptide E and the mRNA (**Fig. 1c**). Nonetheless, the encapsulation efficiency exceeded 85%. Cryogenic transmission electron microscopy (cryo-EM) imaging revealed a spherical morphology for CPE4-LNP, similar to plain LNP, and the majority of both LNPs (>80%) had a diameter of 30-70 nm (**Fig. 1d-e**). The long-term colloidal stability of both LNPs was determined for 10 days and no discernable deviations were observed in either diameter or PDI, indicating that both LNP formulations

were stable over this timeframe (**Fig. 1f**). Upon replacing EGFP-mRNA with Alexa488 labeled nucleic acid, the size distribution and morphology were identical to the EGFP-mRNA encapsulated LNPs (**SI Fig. 2a-2c**). In summary, the addition of 1 mol% of coiled-coil peptide CPE4 to Onpattro LNPs did not change the physicochemical properties of LNPs, thus differences in cell uptake and protein expression can be related to the presence of coiled-coils (*vide infra*).

a

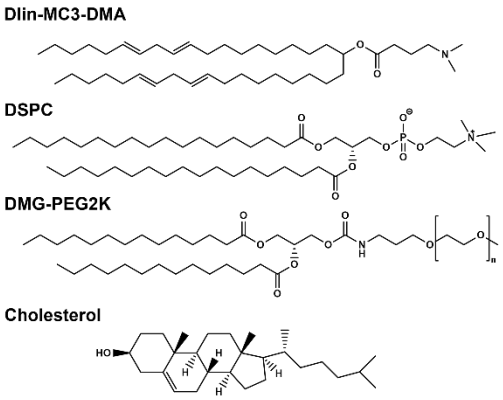

b

Lipid compositions of LNPs (mol%).		
	CPE4-LNP	LNP
Dlin-MC3-DMA	50	50
Cholesterol	37.5	38.5
DSPC	10	10
DMG-PEG2K	1.5	1.5
CPE4	1	

c

Characterization of LNP formulations.				
LNPs	Hydrodynamic diameter (nm)	PDI	Zeta potential (mV)	EE (%)
CPE4-LNP	94.1±2.3	0.167±0.04	-4.37±0.65	85.30±5.14
LNP	80.6±1.8	0.132±0.06	-2.27±0.30	95.13±1.62

d

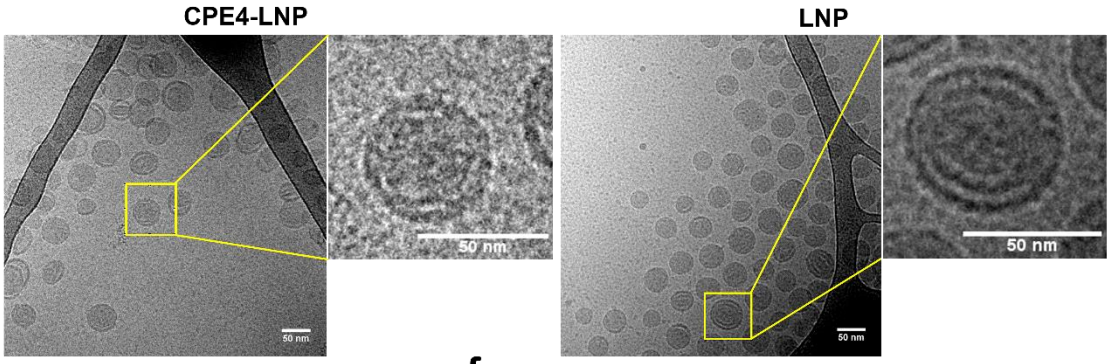

e

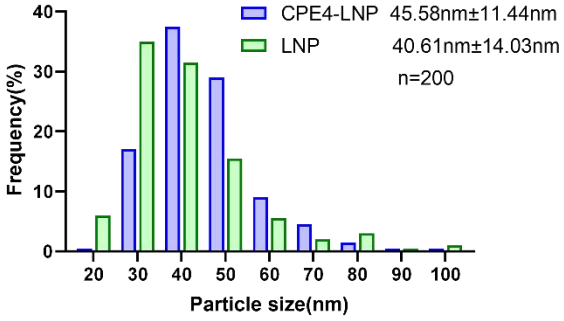

f

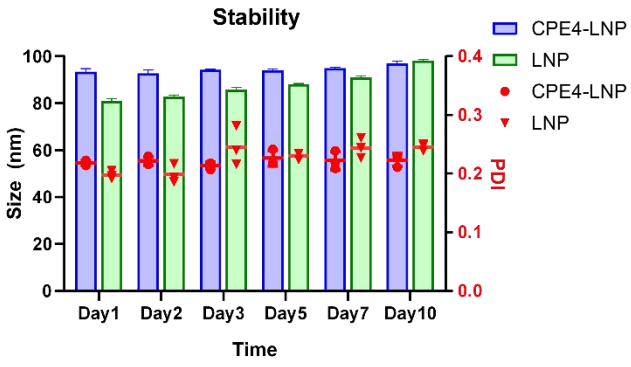

Figure 1. Design and characterization of LNPs carrying EGFP-mRNA. (a) Structures of lipids used for the preparation of LNPs. **(b)** Lipid composition of LNPs (mol %). **(c)** Characterization of LNPs. **(d)** Cryo-EM images of LNPs. Scale bar is 50 nm. **(e)** Size distribution of EGFP-mRNA encapsulated LNPs as determined by cryo-EM. The values were calculated from the size distribution frequency. **(f)** Long-term stability of LNPs. LNPs were stored at 4 °C in PBS buffer. The nanoparticle diameter and PDI were monitored by DLS (mean ± s.d., n = 3).

Cell uptake of LNPs

The uptake of LNPs containing Alexa-488 nucleic acid in HeLa cells and the influence of the E4/K4 coiled-coil pair was studied using confocal microscopy and flow cytometry measurements for qualitative and quantitative analysis (**SI Fig. 3a**). The Onpattro LNP formulation served as a control, and 1 mol % of red-fluorescent PE-LR was added to follow the uptake and location of the lipids. Confocal microscopy imaging revealed that CPK4 decorated HeLa cells induced abundant Alexa488-labeled nucleic acid internalization after only 15 minutes of incubation with CPE4-LNP (**Fig. 2a**). If LNPs enter cells via a process of membrane fusion, it is expected that the lipid dye LR-PE remains mainly bound to the plasma membrane while the content (*i.e.* nucleic acid) enters the cytoplasm.[31,32] Interestingly, colocalization of Alexa488 nucleic acid and LR-PE decreased, indicating that membrane fusion and content nucleic acid release indeed had occurred when using the coiled coils peptides CPE4/CPK4. In contrast, in plain LNP or control experiments in which only one of the coiled-coil peptides was present, only limited nucleic acid and lipid uptake could be detected.

Flow cytometry was used to quantify the cellular uptake of the LNPs. The most efficient uptake was observed when HeLa cells were pretreated with CPK4 and incubated with CPE4-LNP, in accordance with the confocal microscopy study. Within 15 minutes of incubation 99.9% of the cells had nucleic acid internalized, while plain LNP or the control experiments revealed negligible delivery (**Fig. 2b)**. In addition, the mean fluorescence intensity (MFI) analysis of the Alexa488-nucleic acid internalized by cells was significantly higher when coiled-coil peptides were used over all other LNPs (**Fig. 2c-2d**). These results confirmed that the fusogenic coiled-coil system induced rapid and efficient nucleic acid internalization.

To study whether the E4/K4 pair is able to enhance nucleic acid delivery in other cell types, Chinese hamster ovary (CHO), mouse fibroblast NIH/3T3, and human T cell lymphocyte Jurkat cells were transfected with LNPs. Again, CPK4-pretreated cells incubated with CPE4-LNP for 15 minutes resulted in the highest uptake of nucleic acid, regardless of cell type (**Fig. 3a, SI Fig. 3b-3c**). In line with previous experiments in HeLa cells, negligible nucleic acid delivery was observed for plain LNP and all control groups with CHO and NIH/3T3 cells, consistent with flow cytometry data (**Fig. 3b-4c)**. Jurkat cells are regarded as a hard-to-transfect cell line.[33,34-36] By applying our fusogenic coiled-coil peptides, CPK4-pretreated Jurkat cells incubated with CPE4-LNPs produced superior nucleic acid internalization (**Fig. 3a-3c, SI Fig. 3d**), as compared to all other groups, which showed only limited nucleic acid uptake.

Altogether, this cell uptake study confirmed that fusogenic coiled-coil modified LNP can efficiently deliver nucleic acid in high yields to various cell lines as compared to the clinically approved Onpattro LNP formulation.

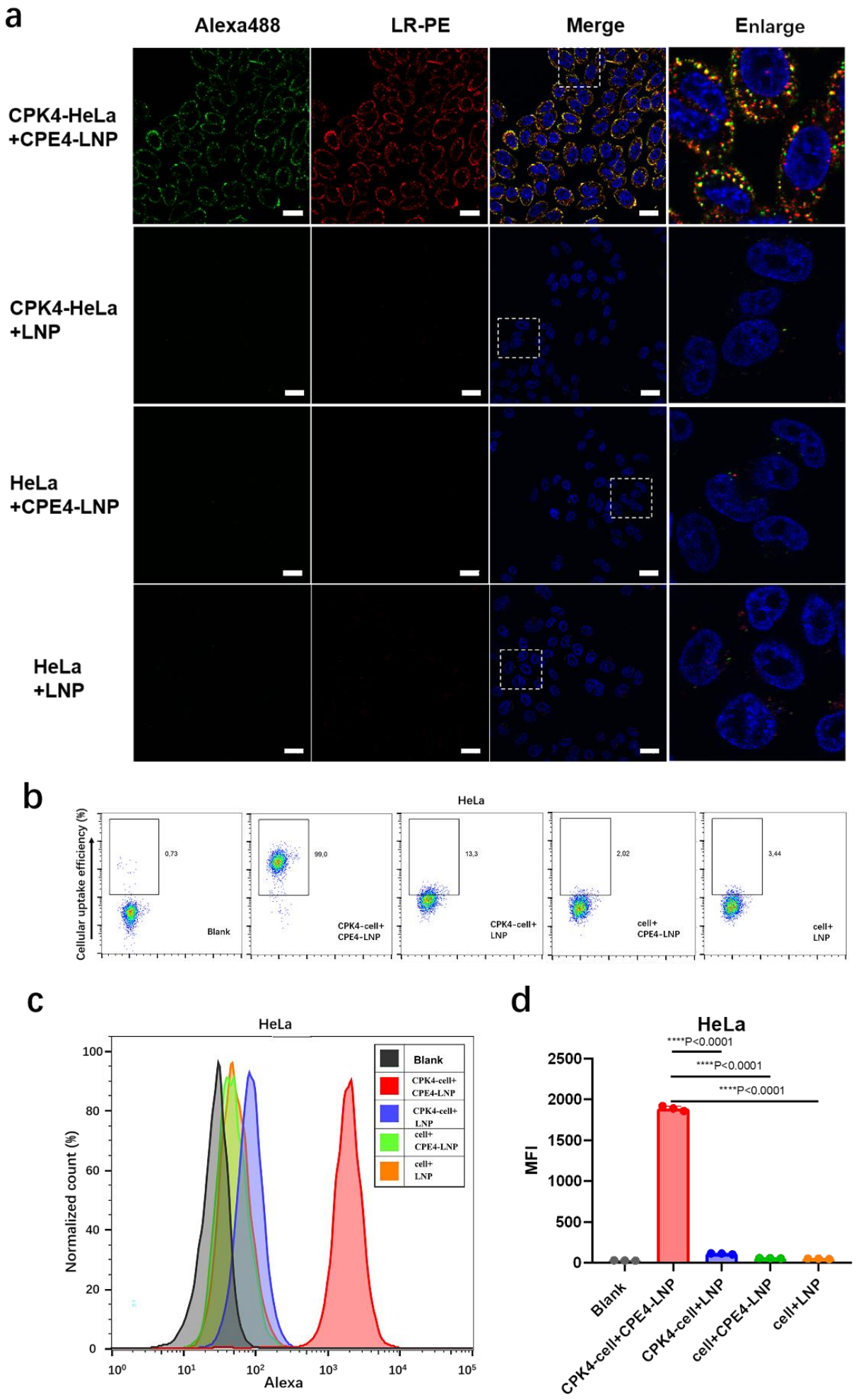
a
Alexa488
LR-PE
Merge
Enlarge
CPK4-HeLa +CPE4-LNP
CPK4-HeLa +LNP
HeLa +CPE4-LNP
HeLa +LNP
b
HeLa
Cellular uptake efficiency (%)
0,73
Blank
99,0
CPK4-cell+ CPE4-LNP
13,3
CPK4-cell+ LNP
2,02
cell+ CPE4-LNP
3,44
cell+ LNP
c
HeLa
Normalized count (%)
Alexa
Blank
CPK4-cell+ CPE4-LNP
CPK4-cell+ LNP
cell+ CPE4-LNP
cell+ LNP
d
HeLa
MFI
****P<0.0001
****P<0.0001
****P<0.0001
Blank
CPK4-cell+CPE4-LNP
CPK4-cell+LNP
cell+CPE4-LNP
cell+LNP

Figure 2. Nucleic acid delivery to HeLa cells using fusogenic coiled-coil LNPs. (a) Confocal microscopy images of cellular internalization of LNPs with HeLa cells. HeLa cells were pretreated with micellar CPK4 (10 μM, 200 μL) for 2 hours. After removal of the supernatant, cells were incubated with CPE4-LNP containing Alexa488-nucleic acid (200 μM, 200 μL) for 15 minutes, washed, and imaged. Blue: Hoechst 33342; green: Alexa488-nucleic acid; red: LR-PE; BF: bright field. Scale bar is 20 μm. **(b)** Cellular internalization efficiency of LNPs with HeLa cells quantified by flow cytometry. **(c-d)** Fluorescence intensity of cells treated with LNPs carrying Alexa488-nucleic acid. An unpaired student t-test was used to determine the significance of the comparisons of data indicated in **d** (*P < 0.05; **P < 0.01; ***P < 0.001; ****P < 0.0001). In all panels, error bars represent the mean ± s.d. (n=3).

Evaluation of lysosome colocalization

Effective nucleic acid internalization and subsequent transfection require efficient escape of the genetic cargo from endosomes/lysosomes into the cytosol.[37,38] However, this is typically an inefficient process, as most of the cargo is not released thus the therapeutic effect is lowered. Therefore novel approaches that facilitate direct cytosolic delivery, and bypass endosomal entrapment, resulting in enhanced transfection efficiency are needed.

Coiled-coil mediated uptake of LNPs was studied as a function of time. For this, CPK4-pretreated cells were incubated with CPE4-LNPs encapsulating fluorescent nucleic acids for 15 minutes and cell uptake was studied. Confocal imaging revealed negligible nucleic acid colocalization with lysosomes during the following 0-8 h, with the majority being dispersed in the cytosol (**Fig. 4a,b**). In contrast, Gilleron *et al* quantified siRNA delivered to cells using LNPs and found that up to 70% was colocalized with lysosomes.[19]

Our data strongly suggests that fusogenic coiled-coil peptides enhance the cellular uptake of LNPs and increase the delivery of genetic cargo to the cytosol of cells, bypassing accumulation in endosomes and lysosomes. Therefore this approach holds promise for efficient transfection of cells with functional mRNA.

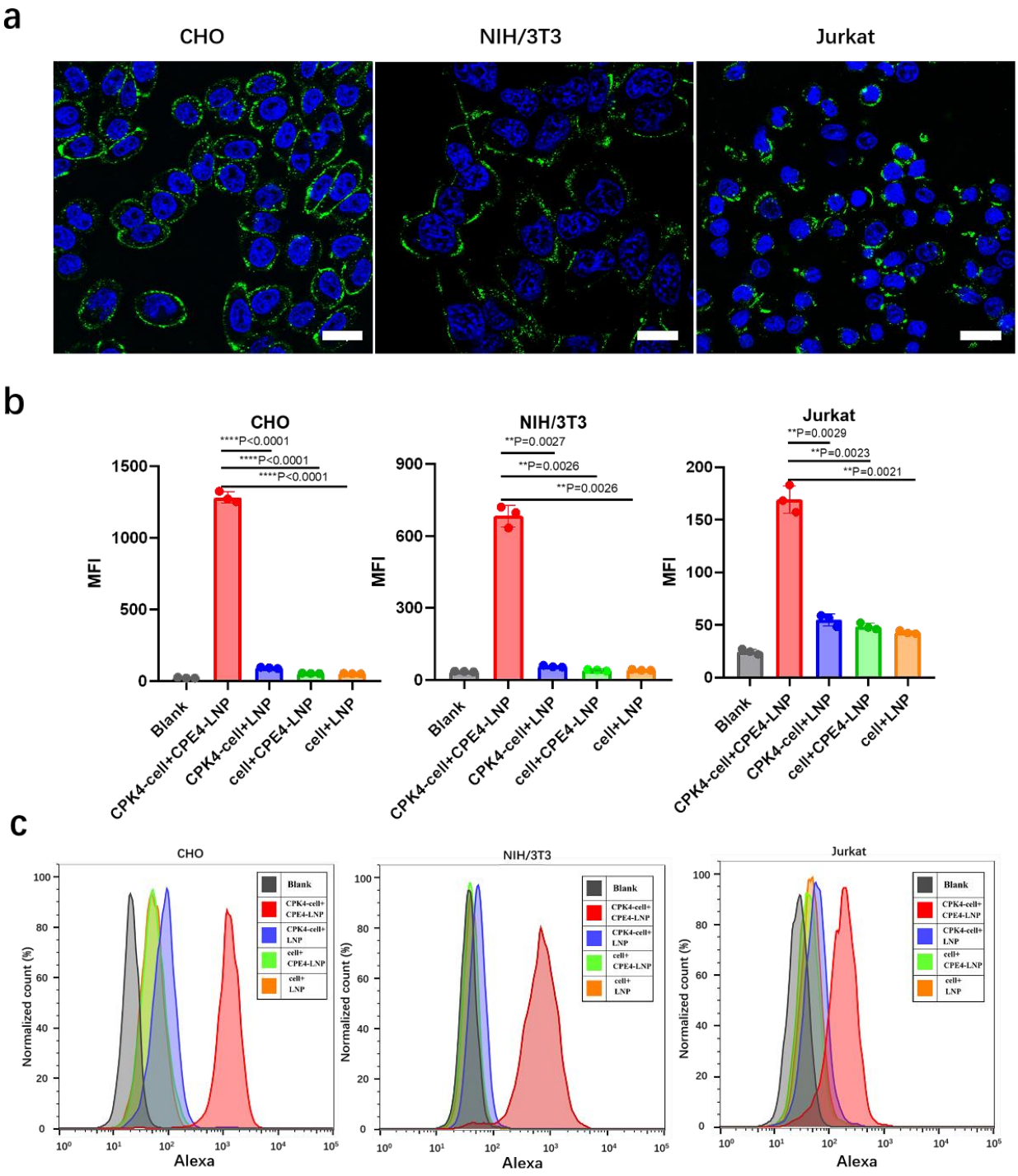

Figure 3. Evaluation of cellular nucleic acid delivery by coiled-coil functionalized LNPs with other cell lines. **(a)** Confocal images of LNPs with CHO, NIH/3T3, and Jurkat cells. Blue: Hoechst 33342; green: Alexa488-nucleic acid. Scale bar is 20 μm. **(b-c)** The fluorescence intensity of internalized LNPs in CHO, NIH/3T3, and Jurkat cells. Alexa488- nucleic acid served as the fluorescent dye. Cells were pretreated with a micellar CPK4 solution (10 μM, 200 μL, 2 h), and after removal of the medium LNPs containing Alexa488-nucleic acid were added (200 μM, 200 μL, 15 min), and the cells were washed again before confocal and flow cytometry measurements. Unpaired student t-test was used to determine the significance of the comparisons of data indicated in **b** (*P < 0.05; **P < 0.01; ***P < 0.001; ****P < 0.0001). In all panels, error bars represent mean ± s.d. (n=3).

Cellular internalization of LNPs

As our fusogenic coiled-coil system appears to facilitate membrane fusion, we wanted to discover whether the internalization mechanism of coiled-coil peptide modified LNPs was different from plain LNPs. Therefore coiled-coil mediated cell uptake of LNPs was studied in the presence of different cellular endocytosis inhibitors (*i.e.* Wortmannin,[39,40] Nocodazole,[41] Pitstop 2,[42] Dynasore,[43,44] Genistein,[45,46] Methyl-β-cyclodextrin (MβCD),[45,47] and Sodium azide[48]).

Cellular internalization of nucleic acid in the presence of endocytosis inhibitors was analyzed by flow cytometry (**Fig. 4c**), and the fluorescence intensity was normalized against the non-inhibitor treated group (control: CPK4-HeLa+CPE4-LNP). None of the endocytosis inhibitors appeared to influence nucleic acid internalization, although incubation at 4°C seemed to decrease the internalization efficiency slightly. Confocal imaging also demonstrated that there was no apparent adverse effects on nucleic acid delivery as the overall distribution in the presence of all tested inhibitors was still comparable to the control group (**SI Fig. 4a**). These results support the hypothesis that the dominant pathway for coiled-coil mediated nucleic acid delivery is independent of endocytosis and is mainly membrane fusion mediated. This pathway avoids endosomal entrapment of genetic cargo and results in enhanced transfection.

For unmodified LNP, cell entry is dependent on endocytic pathways.[38,49] Jerome *et al.* showed that dynasore reduced LNP uptake by around ~75%.[19] Hence, unmodified LNP were evaluated as a contrast to the fusogenic coiled-coil LNP system. As expected, after 4 hours of incubation, flow cytometry and confocal imaging of the cellular uptake of plain LNP showed nucleic acid internalization was remarkably reduced by NaN_3, dynasore, and incubation at 4 °C (**Fig. 4d**, **SI Fig. 4b**). These results confirm that internalization of unmodified LNP is mainly mediated by clathrin-dependent endocytosis.

In summary, while unmodified LNP uptake is mediated by the clathrin-dependent endocytic pathway, our fusogenic coiled-coil LNP system successfully delivered nucleic acid into cells through membrane fusion, avoiding endosomal entrapment of nucleic acid and resulting in enhanced nucleic acid delivery.

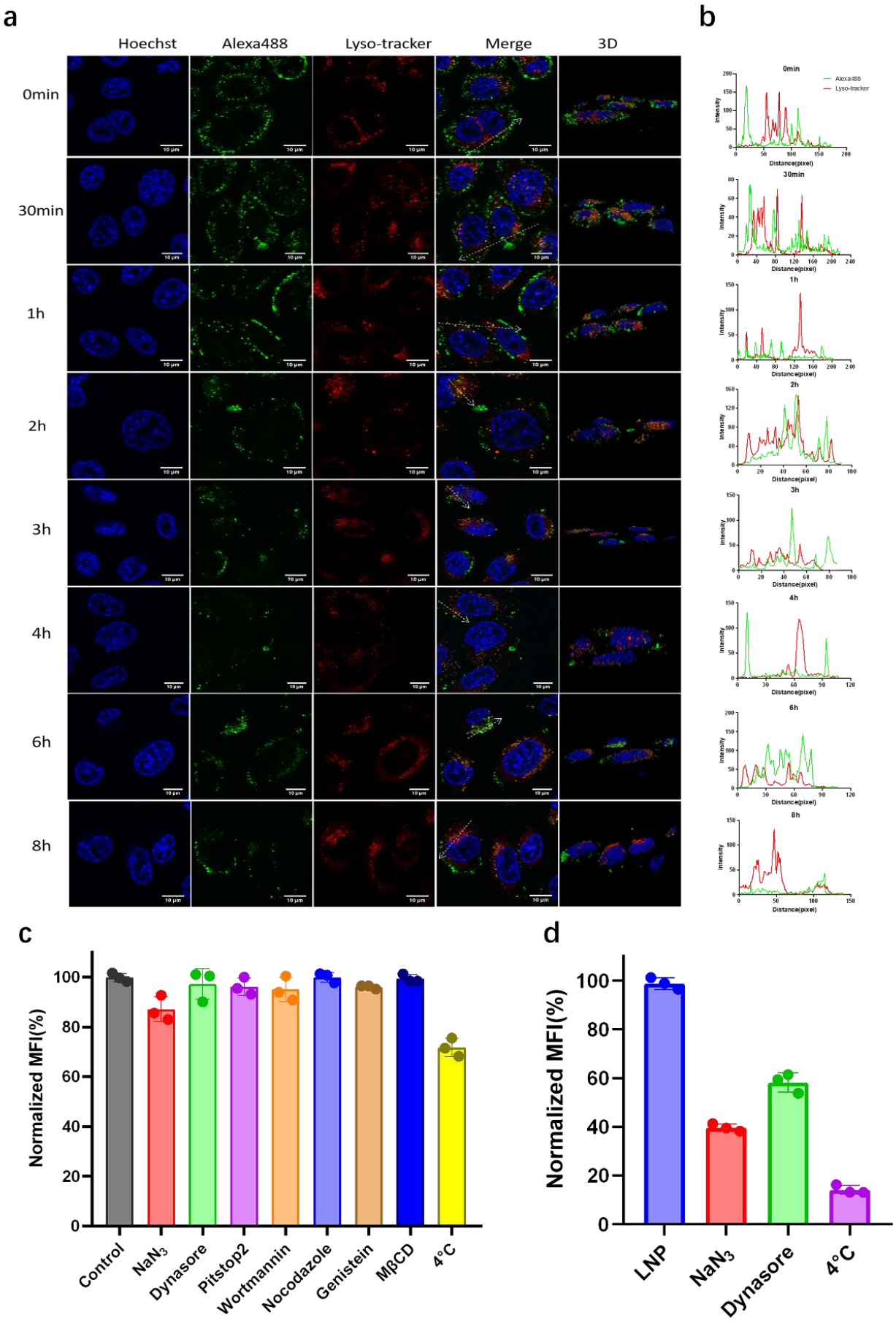
a
Hoechst
Alexa488
Lyso-tracker
Merge
3D
0min
30min
1h
2h
3h
4h
6h
8h
b
Alexa488
Lyso-tracker
Intensity
Distance(pixel)
c
Normalized MFI(%)
Control
NaN3
Dynasore
Pitstop2
Wortmannin
Nocodazole
Genistein
MβCD
4°C
d
Normalized MFI(%)
LNP
NaN3
Dynasore
4°C

Figure 4. Investigation of cellular delivery pathways of LNPs by fusogenic coiled-coil peptides. (a) Confocal images of coiled-coil mediated uptake of LNPs as a function of incubation time in HeLa cells after 15 min uptake; lysosome colocalization is studied by staining lysosomes with lyso-tracker deep red. HeLa cells were pretreated with CPK4 (10 μM, 200 μL) for 2 hours and incubated with CPE4-LNP carrying Alexa488-nucleic acid (200 μM, 200 μL) for 15 min, washed, and replaced by medium. Imaging was performed as a function of time. Blue: Hoechst 33342; green: Alexa488-nucleic acid; red: lyso-tracker deep red. Scale bar is 10 μm. **(b)** Quantitative colocalization analysis of Alexa488-nucleic acid (green curve) and lysosomes (red curve) in the dashed arrow area of the merge channel as a function of time. **(c)** Quantification of Alexa488-nucleic acid delivery to CPK4-pretreated HeLa cells using CPE4-LNP (200 μM, 200 μL) after incubation for 15 min in the presence of various endocytosis inhibitors. Fluorescence intensity was normalized to Alexa-488-nucleic acid delivery in the absence of inhibitors. **(d)** Quantification of cellular internalization efficiency of unmodified LNP (200 μM, 200 μL) after a 4 h incubation period in the presence of various endocytosis inhibitors. Error bars represent mean ± s.d. (n=3).

mRNA Transfection

Gene therapy requires a high transfection efficiency to fulfill successful gene modulating effects. We have shown that fusogenic coiled-coil peptides can improve the delivery of nucleic acids to the cytosol of cells. We then evaluated the transfection performance of the modified LNPs. For this, EGFP-mRNA was encapsulated in LNPs and after transfection, the expression of green fluorescent protein (GFP) was quantified as an easily detectible indicator for functional mRNA delivery. The mRNA concentrations of LNPs were determined by the RiboGreen RNA assay.

Four cell lines were used to study the gene transfection efficiency: HeLa, CHO, NIH/3T3, and Jurkat. Confocal imaging of transfected HeLa cells showed that CPK4-pretreated HeLa cells incubated with CPE4-LNP carrying EGFP-mRNA for 2 hours achieved the highest level of GFP expression, as almost every cell produced strong and uniform GFP expression (**Fig. 5a**). In contrast, the commonly used commercial transfection reagent lipofectamine 3K only transfected a few cells. Onpattro LNP and the control groups that lack one of the peptides achieved only minor GFP expression. Quantitative analysis by flow cytometry confirmed the confocal imaging study (**Fig. 5b**). The fusogenic coiled-coil mediated LNP delivery achieved almost quantitative GFP expression in all cells (99.9%), while lipofectamine 3K mediated transfection resulted in 54.7% GFP positive cells. In addition, all other groups lacking either one or both peptides failed to induce relevant levels of GFP expression. Analysis of the GFP mean fluorescence intensity also illustrated that coiled-coil mediated delivery induced a 50-fold increase in GFP expression as compared to Onpattro LNP and all other groups (**Fig. 5c-5d**). Interestingly, non-CPK4 pretreated HeLa cells incubated with CPE4-LNP induced a reasonable level of GFP-positive cells. However, the MFI in these GFP-positive cells was significantly lower as compared to the fusogenic coiled-coil group. The prolonged incubation time of the cells with CPE4-LNP in this experiment (2 hours) might be the cause for this observation.

Next, transfection of cells with EGFP-mRNA was investigated in other cell lines. CHO and NIH/3T3 cells also showed a robust GFP expression using the fusogenic coiled-coil peptides (**SI Fig. 5a-5d**). Again, the peptide-mediated delivery of mRNA was superior compared to plain LNP or the control groups lacking one of the peptides. Transfection enhancement by the fusogenic coiled-coil LNP system compared to plain LNP was >50-fold in HeLa cells, 63-fold in CHO cells, and 29-fold in NIH/3T3 cells (**SI Fig. 7a-7c**).

Finally, mRNA transfection in T lymphocyte Jurkat cells was studied. Confocal imaging and flow cytometry data revealed that most Jurkat cells became GFP positive and GFP expression intensity (MFI) was highest when the fusogenic coiled-coil peptides were used (**SI Fig. 6a-6d**). Again, transfection was significantly higher when compared to plain LNP or control groups missing one of the peptides. Interestingly, lipofectamine 3K transfection of Jurkat cells was very inefficient. Overall, GFP expression levels in Jurkat were lower compared to HeLa cells, but still, the fusogenic coiled-coil LNP system induced a significant level of transfection enhancement, which was >3-fold higher compared to Onpattro LNP (**SI Fig. 7d**).

In summary, LNP-mediated mRNA delivery using fusogenic coiled-coil peptides is an effective approach to obtaining high levels of protein expression in various cell lines and could act as a potent nonviral vector able to achieve efficient mRNA transfection of cells.

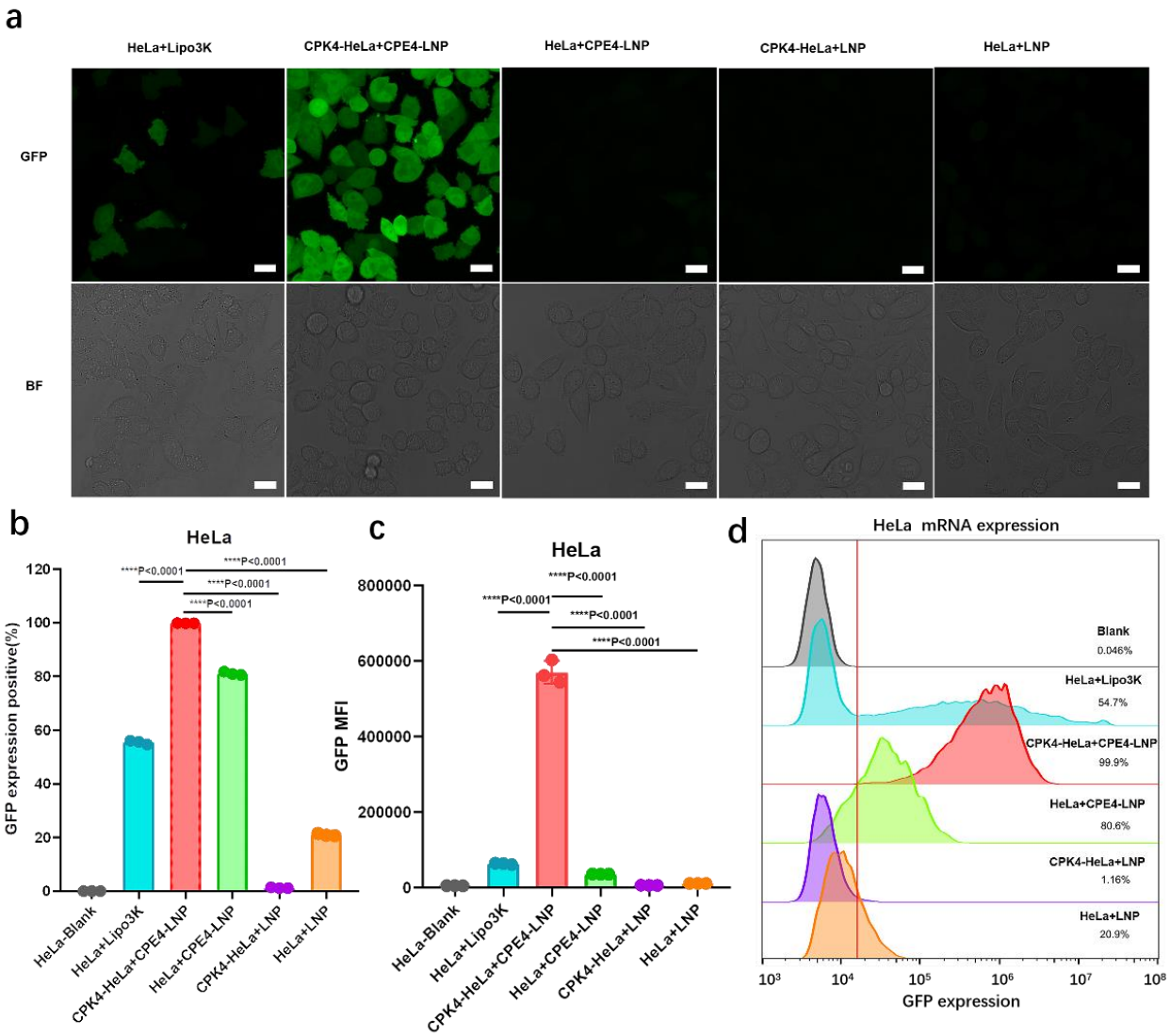

Figure 5. Transfection efficiency of the coiled-coil system with HeLa cells. (a) Confocal images of the EGFP-mRNA transfection of LNPs. Lipo3K: lipofectamine 3K; GFP: green fluorescent protein; BF: bright field. Scale bar is 20 μm. **(b)** The quantification of EGFP-mRNA transfection efficiency of LNPs. **(c-d)** The GFP expression

fluorescence intensity (GFP MFI) of LNPs. HeLa cells were first incubated with CPK4 (10 μM, 200 μL, 2 h), followed by incubation with EGFP-mRNA encapsulated LNPs (1 μg/mL, 2 h). Cells were then washed 3 times and cultured for another 18-24 h before confocal and flow cytometry measurements. Unpaired student t-test was used to determine the significance of the comparisons of data indicated in **b**, and **c**,(*P < 0.05; **P < 0.01; ***P < 0.001; ****P < 0.0001). In all panels, error bars represent mean ± s.d. (n=3).

Cytotoxicity assay of LNPs

For successful nucleic acid-based therapies it is important to keep a balance between transfection efficiency and cytotoxicity of the gene vector. Thus, the expression of GFP was studied as a function of the dose of LNPs carrying EGFP-mRNA, and the cell viability was determined in parallel. Near quantitative GFP expressing cells were obtained at a dose of 1 μg/mL EGFP-mRNA (**SI Fig. 8a**). Next, cell viability after transfection was determined using the cell proliferation reagent WST-1. No significant toxicity was observed at all tested doses of EGFP-mRNA, and cell viability differences between plain LNP and coiled-coil modified LNP were not statistically significant. Interestingly, at higher doses the commercial reagent Lipofectamine 3K was shown to be more toxic (**SI Fig. 8b**). Altogether, these results demonstrate that our coiled-coil gene delivery system achieves potent transfection efficiency without altering the cytotoxicity profile of LNPs.

Discussion and conclusion

Nonviral vectors can be used to encapsulate a wide variety of nucleic acid-based cargoes with a large range of molecular weights, including RNA (e.g. siRNA, mRNA, microRNA, ASO), DNA (*e.g.* plasmids), and genome editing tools (*e.g.* CRISPR/Cas, base editing, prime editing). The delivery of these cargoes using these vectors greatly facilitates precise and permanent correction of diseased genes.[2,50,51] Furthermore, multiple variants can be encapsulated and delivered using the same vector. To date, the design of novel nonviral vectors mainly focuses on establishing effective formulations capable of silencing, correcting, or introducing specific genes with minimal adverse effects.[2,52]

In this study, we showed that fusogenic coiled-coil peptides can induce efficient cellular internalization and potent transfection of nucleic acids *in vitro*. The introduction of 1 mol% of lipopeptide CPE4 to the Onpattro LNP formulation did not alter physicochemical parameters such as size, zeta-potential, and mRNA encapsulation efficiency. However, CPE4 exerted a significantly enhanced internalization and transfection effect when target cells were pretreated with the complementary lipopeptide CPK4. Qualitative evaluation of transfection with confocal microscopy and quantitative analysis with flow cytometry revealed efficient nucleic acid uptake within 15 minutes of incubation when the fusogenic coiled-coil peptides were used. In contrast, plain LNP and all control groups were unable to deliver measurable amounts of nucleic acid within this time frame. Coiled-coil mediated LNP transfection to cells is fast (within 2 hours of incubation) when compared to other cationic and lipid nanoparticles; these typically require longer incubation times (up to 24-72 h) to obtain significant transfection.[53,54] Furthermore we confirmed that the coiled-coil system is functional on various cell lines including CHO and the hard to transfect Jurkat cells.

Gene delivery into cells using non-viral vectors often suffers from a poor ability to escape from the endosomal and/or lysosomal compartments. For siRNA, the endosomal escape was determined to be around 1-2%, making delivery very inefficient and thus lowering the potential therapeutic effect.[19]

This is because endosomal escape is often spatio-temporally limited and only occurs in the brief stage of endo-lysosomal maturation.[19,38] Various approaches have been investigated to enhance endosomal escape efficiency, examples are the introduction of cell-penetrating peptides,[23,24] endosome disrupting peptides,[24,55] and photochemical internalization.[56,57] However, these approaches typically lack cell selectivity[58] and cause membrane destruction[57] resulting in cytotoxicity.[59,60] Using fusogenic coiled-coil peptides we managed to circumvent endosomal entrapment, resulting in direct cytosolic delivery of nucleic acid. This direct delivery was proven by performing uptake studies in the presence of common endocytosis inhibitors and quantifying the fraction of nucleic acid inside CPE4-LNP localized in lysosomes. Transfection of cells with EGFP-mRNA using fusogenic coiled-coil peptides resulted in an enhanced transfection performance as shown by the near-quantitative number of GFP positive cells and the high expression level of GFP in these cells as compared to plain LNP (up to a 63-fold increase in GFP expression). Furthermore, the control studies revealed that both coiled-coil peptides are required for efficient transfection, highlighting the importance of the coiled-coil interaction for the delivery of mRNA and concomitant protein expression. Our approach also outperformed the commercial reagent lipofectamine 3K in all studies. Thus using fusogenic coiled-coil peptides lowers the amount of mRNA required to reach a desired expression level, which is also beneficial for cell viability. In this study, EGFP-mRNA was used, but any other nucleic acid could be delivered in a similar fashion.

The current approach requires pretreatment of cells with CPK4, rendering it impractical for *in vivo* applications via systemic administration. Nevertheless, *in vitro*/*ex vivo* delivery and other *in vivo* delivery approaches other than *i.v.* injections, such as local/subcutaneous injections may be feasible. A potential application could be adoptive cell therapy.[61,62,63] Except for viral transduction, other attempts of lymphocyte transfection often apply electroporation and nucleofection to deliver exogenous genes into T cells,[64,65] but it requires specialized equipment, disrupts membrane, produces cytokine, causes cytoplasmic content loss and cytotoxicity, and unable to penetrate membrane across cells consistently.[66,67] Coiled-coil mediated LNP delivery might also be applicable to the gene-editing field, such as CRISPR/Cas9 editing[68,69] and prime gene editing.[70] The highly efficient, transient, non-integrating Cas9 expression could greatly reduce the off-target effects, immune responses, and integration into the genome, which could be accomplished by our nonviral fusogenic coiled-coil delivery system.

In conclusion, fusogenic coiled-coil peptides can significantly enhance the delivery of nucleic acid to cells using LNPs. By circumventing the endosomal pathway, the genetic cargo is delivered to the cytosol of cells. For EGFP-mRNA this resulted in an up to a 63-fold increase in protein expression as compared to unmodified LNP, opening new avenues for nucleic acids based therapies. Furthermore, we showed efficient transfection in various cell lines with substantial improvement as compared to the commercial transfection reagent lipofectamine 3K. Thus modification of LNPs with fusogenic coiled-coil peptides could serve as a promising strategy to enhance LNP efficacy to deliver nucleic acid based therapies *in vitro, ex vivo,* and potentially *in vivo*.

Methods

Chemicals.

All Fmoc-protected amino acids were purchased from Novabiochem. Piperidine, trifluoroacetic acid, acetonitrile, dimethylformamide (DMF) were purchased from Biosolve; dichloromethane (DCM), and ethanol were purchased from Sigma-Aldrich. 1,2-distearoyl-*sn*-glycero-3-phosphocholine (DSPC), 1,2-dimyristoyl-*rac*-glycero-3-methoxypolyethylene glycol-2000 (DMG-PEG2K), 1,2-dioleoyl-*sn*-glycero-3-phosphocholine (DOPC), 1,2-dioleoyl-*sn*-glycero-3-phosphoethanolamine (DOPE), 1,2-dioleoyl-*sn*-glycero-3-phosphoethanolamine-N-(7-nitro-2-1,3-benzoxadiazol-4-yl) (PE-NBD), 1,2-dioleoyl-*sn*-glycero-3-phosphoethanolamine-N-(lissamine rhodamine B sulfonyl) (PE-LR), were purchased from Avanti Polar Lipids, DLin-MC3-DMA was purchased from Biorbyt (Cambridge, England), and dynasore, wortmannin, nocodazole, pitstop2, genistein, methyl-β-cyclodextrin (MβCD), sodium azide (NaN_3), cholesterol was purchased from Sigma-Aldrich. Lyso-tracker deep red was purchased from Thermofisher. Triton™ X-100 was purchased from Acros Organics. QuantiT™ RiboGreen® RNA reagent and rRNA standards were purchased from Life Technologies. WST-1 reagent was purchased from Sigma-Aldrich. Nucleic acid: Alexa488-nucleic acid (Alexa488-5'-AACCATACACCTACTACCTCA-3') was purchased from Integrated DNA technology; cleancap EGFP-mRNA was purchased from Trilink biotechnology.

Lipopeptide synthesis and purification.

Peptide E3 $(EIAALEK)_3$, K3 $(KIAALKE)_3$, E4 $(EIAALEK)_4$ and K4 $(KIAALKE)_4$ were synthesized using Fmoc chemistry and standard solid-phase peptide synthesis protocols on a 0.1 mmol scale as described previously.[28] Fmoc deprotection was performed using 20% piperidine in DMF at 90 °C for 60 s. Amide coupling was achieved using 5 eq. of protected amino acid, 5 eq. DIC as activator and 5 eq. Oxyma as activator base, heated at 95 °C for 240 seconds. Lipidated peptides (CPK3, CPE3, CPK4, CPE4) were made on resin via the coupling of 2.5 equivalents of N_3- PEG_4-COOH, with 2.5 eq of HBTU and 5 eq. of DIPEA in DMF overnight at room temperature. After washing the resin with DMF, the azide was reduced using 10 eq. of PME3 (1 M in toluene), with 4:1 dioxane:water as solvent for 2.5 hours. The resin was then washed thoroughly with 4:1 dioxane:water, MeOH and DMF. Lipidation was achieved using 2 eq. cholesteryl hemisuccinate, 2 eq. HBTU and 4 eq. DIPEA in 1:1 DMF:DCM. After the final coupling the resin was washed with DMF, MeOH, and DCM, dried under vacuum, and the peptide was cleaved using a mixture of TFA:TIPS:EDDT:water (92.5:2.5:2.5:2.5) for 1 hour, after which the peptide was precipitated in cold diethyl ether, collected via centrifugation and lyophilized. All peptides were purified by HPLC on a Shimadzu system consisting of two KC-20AR pumps and an SPD-20A or SPD-M20A detector equipped with a Kinetix Evo C18 column. Eluents consisted of 0.1% TFA in water (A) and 0.1% TFA in MeCN (B), with all peptides eluted using a gradient of 20-90% B over 35 minutes, with a flow rate of 12 mL/min. Collected fractions were checked for purity via LC-MS, with the pure fractions being pooled and lyophilized. LC-MS spectra were recorded using a Thermo Scientific TSQ quantum access MAX mass detector connected to an Ultimate 3000 liquid chromatography system fitted with a 50x4.6 mm Phenomenex Gemini 3 μm C18 column.

Lipid nanoparticles formulation.

Lipids and lipopeptides were combined at the desired molar ratios and concentrations from stock solutions dissolved in chloroform:methanol (1:1). Solvents were evaporated under a nitrogen flow

and residual solvent was removed *in vacuo* for at least 30 minutes. The lipid film was dissolved in absolute ethanol and used for assembly (total [lipid] was 1 μmol). A solution of mRNA was made by diluting nucleic acid (Alexa488-nucleic acid or EGFP-mRNA) in 50 mM citrate buffer (pH = 4, RNase free H_2O). The solutions were loaded into two separate syringes and connected to a T-junction microfluidic mixer. The solutions were mixed in a 3:1 flow ratio of nucleic acid:lipids (1.5 mL/min for the nucleic acid solution, 0.5 mL/min for the lipids solution, N/P ratio was 16:1). After mixing, the solution was directly loaded in a 20 k MWCO dialysis cassette (Slide-A-Lyzer™, Thermo Scientific) and dialyzed against 1 x PBS overnight. After overnight dialysis, mRNA encapsulation efficiency was determined by Quant-iT™ RiboGreen™ RNA Assay Kit as described below. For confocal cellular uptake experiments, 1 mol% of PE-LR was added with the other lipids.

Biophysical characterization.
The size and zeta potential of LNPs were measured using a Malvern zetasizer Nano ZS. Long term stability of LNPs was assessed by measuring the hydrodynamic radius using DLS for 10 days.

The morphology of LNPs was analyzed by cryogenic transmission electron microscopy (cryo-EM). Vitrification of concentrated LNPs (lipids ~10 mM) was performed using a Leica EM GP operating at 21 °C and 95 % room humidity (RH). Sample suspensions were placed on glow discharged 100 μm lacey carbon film supported on 200 mesh copper grids (Electron Microscopy Sciences). Optimal results were achieved using a 60-second pre-blot and a 1-second blot time. After vitrification, sample grids were maintained below -170 °C, and imaging was performed on a Tecnai T12 (Thermo Fisher) with a biotwin lens and LaB6 filament operating at 120 keV equipped with an Eagle 4 K×4 K CCD camera (Thermo Fisher). Images were acquired at a nominal underfocus of -2 to -3 μm (49,000× magnification) with an electron dose of ~2000 e/nm2. The size distribution of LNPs was based on 100 particles (Fiji ImageJ) from cryo images normalized by percentage distribution.

Circular dichroism measurements: CD spectra were recorded on a JASCO J-815 CD spectrometer fitted with a Peltier temperature controller. Unless otherwise specified, samples were measured at 20 °C in a quartz cuvette with a 2 mm path length. Spectra were recorded from 200 to 250 nm at 1 nm intervals, with a bandwidth of 1 nm, with the final spectrum consisting of the average of 5 sequentially recorded spectra. The mean residue molar ellipticity (θ, deg cm^2 $dmol^{-1}$) was calculated according to equation ($[\theta] = (100 * [\theta]obs\ )/(c * n * l)$), [θ]obs representing the observed ellipticity in mdeg, c the peptide concentration in mM, n the number of peptide bonds and l the path length of the cuvette in cm.

mRNA encapsulation efficiency.
The encapsulation efficiency (EE%) of EGFP-mRNA was measured using a Quant-iT™ RiboGreen™ RNA Assay Kit (Invitrogen). For the determination of non-encapsulated EGFP-mRNA, LNPs after dialysis were diluted with 1 x TE buffer (RNase free) and treated with the RiboGreen™ reagent. For the determination of the total amount of EGFP-mRNA, LNPs after dialysis were treated with 1% Triton X-100 in TE buffer (RNase free) and incubated for 5 minutes followed by dilution with TE buffer and treatment with the RiboGreen™ reagent. The supplied RNA standards were used to generate a standard curve and changes in fluorescence was measured in 96-well plates using a TECAN Infinite M1000 Pro microplate reader. The percentage of mRNA encapsulation (EE%) was determined using the fraction of (Ftotal RNA – Ffree RNA)/Ftotal RNA * 100%.

Cell culture, and cell uptake study.

Cell culture: HeLa, CHO, NIH/3T3, and Jurkat cell lines purchased from ATCC were cultured according to ATCC guidelines. The DMEM and RPMI-1640 growth media (Sigma Aldrich) containing sodium bicarbonate, without sodium pyruvate and HEPES, were supplemented with 10% fetal bovine serum (Sigma), 1% L-glutamine (Thermo Fisher Scientific), and 1% penicillin/streptomycin (Thermo Fisher Scientific). HeLa, CHO, and NIH/3T3 were cultured with DMEM medium, and Jurkat was cultured with RPMI-1640 medium, at 37 °C in the presence of 5% CO_2.

Cell uptake (flow cytometry measurements): Flow cytometry analysis (FACs) of cellular uptake efficiency was performed to compare internalization efficiency differences. All lipids with a certain ratio (molar ratio DOPC:DOPE:cholesterol=2:1:1, 1 mol% of NBD-PE) were dried under N_2 flow, hydrated with PBS and sonicated at 55°C for 3 min. The CPE and CPK modified liposomes (CPE3-lipo, CPE4-lipo, CPK3-lipo, and CPK4-lipo) were made the same way while adding 1 mol% of CPE3, CPE4, CPK3, and CPK4 into the lipid mixture. CPK3, CPK4, CPE3, CPE4 lipid films were made, hydrated with complete DMEM, and sonicated for 10 min at room temperature. For cellular uptake efficiency tests, HeLa cells were pretreated with CPK3, CPK4, CPE3, CPE4 in DMEM for 2 h, then NBD labeled liposomes CPE3-lipo, CPE4-lipo, CPK3-lipo, and CPK4-lipo were added to the cells (15 min). After 15 min incubation, the medium was removed and cells were washed with PBS, digested with trypsin, washed, and resuspended in PBS, followed by flow cytometry measurements. For the cellular internalization efficiency of CPE3-LNP and CPE4-LNP, both LNPs were prepared as previously described by encapsulating Alexa488 nucleic acid, 1 mol% of CPE3 and CPE4 lipopeptides were added to the other lipids, and then proceeded to form LNPs, as described above, was followed.

Cell uptake (confocal imaging): Cells were seeded in an 8-well confocal slide at a density of $5*10^4$ cells/well and incubated at 37 °C in 5% CO_2, and after 18 h, the medium was removed and medium containing CPK4 (10 μM, 200 μL) and Hoechst 33342 (5 μM, 200 μL) was added and incubated for 2 h at 37 °C in 5% CO_2. Next, cells were washed with PBS (3X), and incubated with CPE4-LNP (200 μM, 200 μL) containing Alexa488 labeled nucleic acid for 15 min. The supernatant was removed and cells were washed with PBS, and DMEM free of phenol red indicator was added for confocal microscopy measurements using a Leica TCS SP8 confocal laser scanning microscope. For flow cytometry measurements, cells were seeded in 24-well plates at a density of $2.5*10^5$ cells/well, the rest of the procedure was the same as for the confocal measurements.

Endocytosis inhibitor assay (confocal imaging): HeLa cells were pretreated with nocodazole (40 μM), wortmannin (0.25 μM), dynasore (80 μM), pitstop2 (20 μM), genistein (200 μM), methyl-β-cyclodextrin (MβCD, 10 mM) or sodium azide (0.1% w/v) in DMEM medium for 1 h, after which the medium was replaced with medium containing lyso-tracker deep red (75 nM), CPK4 (10 μM), and fresh inhibitors and incubated for 2 h, then Alexa488 nucleic acid encapsulated CPE4-LNP (200 μM) were incubated in the presence of the inhibitors. After 15 min, the cells were washed three times, and phenol red indicator free DMEM was added for confocal microscopy imaging. When performing cellular uptake assays at 4 °C, cells were first incubated with lyso-tracker deep red (75 nM) and CPK4 (10 μM) for 2 h at 37 °C, then 1 h at 4 °C. The medium was removed and cells were washed and incubated for 15 min at 4 °C in the presence of CPE4-LNP (200 μM), followed by confocal imaging.

Endocytosis inhibitor assay (flow cytometry measurements): Cells were seeded on 24-well plates at a density of $2.5*10^5$ cells/well. After 18 h, the medium was removed and cells were incubated with inhibitors and CPK4 in medium (10 μM) for 2 h. Then Alexa488 nucleic acid encapsulated CPE4-LNP (200 μM, 15 min) was added in the presence of fresh inhibitors. The cells were washed, digested, and flow cytometry measurements using a Guava easyCyte machine (Luminex Corporation) were performed.

For the endocytosis pathway assay of unmodified LNPs, the cells were preincubated with endocytosis inhibitors for 2 h, then LNPs were added to the cells in the presence of fresh inhibitors and incubated for 4 h, and washed before the confocal imaging and flow cytometry measurements.

Lysosome colocalization study.
HeLa cells were seeded on 8-well confocal plates at a density of $5*10^4$cells/well. After overnight growth the cells were treated with lyso-tracker deep red (75 nM) and CPK4 (10 μM) for 2 h. The supernatant was removed, and Alexa488 nucleic acid encapsulated CPE4-LNP (200 μM) was added and incubated for 15 min. The medium was removed, and lyso-tracker deep red (75 nM) in DMEM was added and incubated at different times before confocal imaging.

Transfection assay.
CPE4-LNPs and LNPs encapsulating EGFP-mRNA were prepared as described previously. HeLa, CHO, NIH/3T3, and Jurkat were cultured in 8-well confocal plates at the density of $2*10^4$ cells/well overnight before cells were pretreated with CPK4-medium (10 μM) for 2 h, washed three times with PBS, then LNPs (1 μg/mL) were added to the cells and incubated for 2 h, then the medium was removed and washed three times, refreshed with fresh medium for continuous 18-24 h culturing before confocal imaging and flow cytometry measurements. The concentration of LNPs was determined by Quant-iT Ribogreen RNA assay. The commercial transfection agent lipofectamine 3K/EGFP-mRNA was prepared according to the manufacturers protocol using the same amount of EGFP-mRNA, and cells were transfected for 2 h and refreshed with medium before 18-24 h culturing.

Cell viability measurements.
HeLa cells were seeded on 96-well plates at a density of $1*10^4$ cells per well overnight, then the same procedure as previously described was followed but different concentrations of LNPs (0.25 μg/mL, 0.5 μg/mL, 1 μg/mL, 1.5 μg/mL, 2 μg/mL) were added. After 24 h incubation, cell proliferation reagent WST-1 solution (20 μL, Sigma-Aldrich) was added to the medium (200 μL) and cells were incubated for another 4 h at 37 °C. The absorbance at 450 nm was measured at room temperature using a Tecan infinite M1000. The cell viability was normalized with a control (blank HeLa cells), which was set at 100% cell survival.

Statistical analysis.
All experiments were performed in triplicate (n=3) unless specified otherwise, and the significance was determined using an unpaired student t-test (Graphpad Prism) for all comparisons. *$p \leq 0.05$, **$p \leq 0.01$, ***$p \leq 0.001$, ****$P < 0.0001$.

References

1. Akinc, A.; Maier, M. A.; Manoharan, M.; Fitzgerald, K.; Jayaraman, M.; Barros, S.; Ansell, S.; Du, X.; Hope, M. J.; Madden, T. D.; Mui, B. L.; Semple, S. C.; Tam, Y. K.; Ciufolini, M.; Witzigmann, D.; Kulkarni, J. A.; van der Meel, R.; Cullis, P. R., The Onpattro story and the clinical translation of nanomedicines containing nucleic acid-based drugs. *Nature Nanotechnology* **2019,** *14* (12), 1084-1087.

2. Yin, H.; Kanasty, R. L.; Eltoukhy, A. A.; Vegas, A. J.; Dorkin, J. R.; Anderson, D. G., Non-viral vectors for gene-based therapy. *Nature Reviews Genetics* **2014,** *15* (8), 541-555.

3. Guan, S.; Rosenecker, J., Nanotechnologies in delivery of mRNA therapeutics using nonviral vector-based delivery systems. *Gene Therapy* **2017,** *24* (3), 133-143.

4. Naldini, L., Gene therapy returns to centre stage. *Nature* **2015,** *526* (7573), 351-360.

5. Somia, N.; Verma, I. M., Gene therapy: trials and tribulations. *Nature Reviews Genetics* **2000,** *1* (2), 91-99.

6. Li, C.; Samulski, R. J., Engineering adeno-associated virus vectors for gene therapy. *Nature Reviews Genetics* **2020,** *21* (4), 255-272.

7. Kuzmin, D. A.; Shutova, M. V.; Johnston, N. R.; Smith, O. P.; Fedorin, V. V.; Kukushkin, Y. S.; van der Loo, J. C., The clinical landscape for AAV gene therapies. *Nature Reviews Drug Discovery* **2021,** *20* (3), 173-175.

8. Dunbar, C. E.; High, K. A.; Joung, J. K.; Kohn, D. B.; Ozawa, K.; Sadelain, M., Gene therapy comes of age. *Science* **2018,** *359* (6372), eaan4672.

9. Thomas, C. E.; Ehrhardt, A.; Kay, M. A., Progress and problems with the use of viral vectors for gene therapy. *Nature Reviews Genetics* **2003,** *4* (5), 346-358.

10. Bessis, N.; GarciaCozar, F. J.; Boissier, M. C., Immune responses to gene therapy vectors: influence on vector function and effector mechanisms. *Gene Therapy* **2004,** *11* (1), S10-S17.

11. Sabnis, S.; Kumarasinghe, E. S.; Salerno, T.; Mihai, C.; Ketova, T.; Senn, J. J.; Lynn, A.; Bulychev, A.; McFadyen, I.; Chan, J.; Almarsson, Ö.; Stanton, M. G.; Benenato, K. E., A Novel Amino Lipid Series for mRNA Delivery: Improved Endosomal Escape and Sustained Pharmacology and Safety in Non-human Primates. *Molecular Therapy* **2018,** *26* (6), 1509-1519.

12. Witzigmann, D.; Kulkarni, J. A.; Leung, J.; Chen, S.; Cullis, P. R.; van der Meel, R., Lipid nanoparticle technology for therapeutic gene regulation in the liver. *Advanced Drug Delivery Reviews* **2020,** *159*, 344-363.

13. Zhao, Y.; Zheng, Z.; Cohen, C. J.; Gattinoni, L.; Palmer, D. C.; Restifo, N. P.; Rosenberg, S. A.; Morgan, R. A., High-Efficiency Transfection of Primary Human and Mouse T Lymphocytes Using RNA Electroporation. *Molecular Therapy* **2006,** *13* (1), 151-159.

14. Slivac, I.; Guay, D.; Mangion, M.; Champeil, J.; Gaillet, B., Non-viral nucleic acid delivery methods. *Expert Opinion on Biological Therapy* **2017,** *17* (1), 105-118.

15. Do, H. D.; Couillaud, B. M.; Doan, B.-T.; Corvis, Y.; Mignet, N., Advances on non-invasive physically triggered nucleic acid delivery from nanocarriers. *Advanced Drug Delivery Reviews* **2019,** *138*, 3-17.

16. Zhang, Y.; Sun, C.; Wang, C.; Jankovic, K. E.; Dong, Y., Lipids and Lipid Derivatives for RNA Delivery. *Chemical Reviews* **2021,** *121* (20), 12181-12277.

17. Yonezawa, S.; Koide, H.; Asai, T., Recent advances in siRNA delivery mediated by lipid-based nanoparticles. *Advanced Drug Delivery Reviews* **2020,** *154-155*, 64-78.

18. Kowalski, P. S.; Rudra, A.; Miao, L.; Anderson, D. G., Delivering the Messenger: Advances in Technologies for Therapeutic mRNA Delivery. *Molecular Therapy* **2019,** *27* (4), 710-728.

19. Akinc, A.; Querbes, W.; De, S.; Qin, J.; Frank-Kamenetsky, M.; Jayaprakash, K. N.; Jayaraman, M.; Rajeev, K. G.; Cantley, W. L.; Dorkin, J. R.; Butler, J. S.; Qin, L.; Racie, T.; Sprague, A.; Fava, E.; Zeigerer, A.; Hope, M. J.; Zerial, M.; Sah, D. W. Y.; Fitzgerald, K.; Tracy, M. A.; Manoharan, M.;

Koteliansky, V.; Fougerolles, A. d.; Maier, M. A., Targeted Delivery of RNAi Therapeutics With Endogenous and Exogenous Ligand-Based Mechanisms. *Molecular Therapy* **2010,** *18* (7), 1357-1364.
20. Wittrup, A.; Ai, A.; Liu, X.; Hamar, P.; Trifonova, R.; Charisse, K.; Manoharan, M.; Kirchhausen, T.; Lieberman, J., Visualizing lipid-formulated siRNA release from endosomes and target gene knockdown. *Nature Biotechnology* **2015,** *33* (8), 870-876.
21. Gilleron, J.; Querbes, W.; Zeigerer, A.; Borodovsky, A.; Marsico, G.; Schubert, U.; Manygoats, K.; Seifert, S.; Andree, C.; Stöter, M.; Epstein-Barash, H.; Zhang, L.; Koteliansky, V.; Fitzgerald, K.; Fava, E.; Bickle, M.; Kalaidzidis, Y.; Akinc, A.; Maier, M.; Zerial, M., Image-based analysis of lipid nanoparticle–mediated siRNA delivery, intracellular trafficking and endosomal escape. *Nature Biotechnology* **2013,** *31* (7), 638-646.
22. Paramasivam, P.; Franke, C.; Stöter, M.; Höijer, A.; Bartesaghi, S.; Sabirsh, A.; Lindfors, L.; Arteta, M. Y.; Dahlén, A.; Bak, A.; Andersson, S.; Kalaidzidis, Y.; Bickle, M.; Zerial, M., Endosomal escape of delivered mRNA from endosomal recycling tubules visualized at the nanoscale. *Journal of Cell Biology* **2021,** *221* (2), e202110137.
23. Degors, I. M. S.; Wang, C.; Rehman, Z. U.; Zuhorn, I. S., Carriers Break Barriers in Drug Delivery: Endocytosis and Endosomal Escape of Gene Delivery Vectors. *Accounts of Chemical Research* **2019,** *52* (7), 1750-1760.
24. Zhu, J.; Qiao, M.; Wang, Q.; Ye, Y.; Ba, S.; Ma, J.; Hu, H.; Zhao, X.; Chen, D., Dual-responsive polyplexes with enhanced disassembly and endosomal escape for efficient delivery of siRNA. *Biomaterials* **2018,** *162*, 47-59.
25. Endoh, T.; Ohtsuki, T., Cellular siRNA delivery using cell-penetrating peptides modified for endosomal escape. *Advanced Drug Delivery Reviews* **2009,** *61* (9), 704-709.
26. Wang, Y.-H.; Hou, Y.-W.; Lee, H.-J., An intracellular delivery method for siRNA by an arginine-rich peptide. *Journal of Biochemical and Biophysical Methods* **2007,** *70* (4), 579-586.
27. Chen, Y. A.; Scheller, R. H., SNARE-mediated membrane fusion. *Nature Reviews Molecular Cell Biology* **2001,** *2* (2), 98-106.
28. Jahn, R.; Scheller, R. H., SNAREs — engines for membrane fusion. *Nature Reviews Molecular Cell Biology* **2006,** *7* (9), 631-643.
29. Yang, J.; Bahreman, A.; Daudey, G.; Bussmann, J.; Olsthoorn, R. C. L.; Kros, A., Drug Delivery via Cell Membrane Fusion Using Lipopeptide Modified Liposomes. *ACS Central Science* **2016,** *2* (9), 621-630.
30. Yang, J.; Shimada, Y.; Olsthoorn, R. C. L.; Snaar-Jagalska, B. E.; Spaink, H. P.; Kros, A., Application of Coiled Coil Peptides in Liposomal Anticancer Drug Delivery Using a Zebrafish Xenograft Model. *ACS Nano* **2016,** *10* (8), 7428-7435.
31. Kong, L.; Askes, S. H. C.; Bonnet, S.; Kros, A.; Campbell, F., Temporal Control of Membrane Fusion through Photolabile PEGylation of Liposome Membranes. *Angewandte Chemie International Edition* **2016,** *55* (4), 1396-1400.
32. Kulkarni, J. A.; Witzigmann, D.; Leung, J.; van der Meel, R.; Zaifman, J.; Darjuan, M. M.; Grisch-Chan, H. M.; Thöny, B.; Tam, Y. Y. C.; Cullis, P. R., Fusion-dependent formation of lipid nanoparticles containing macromolecular payloads. *Nanoscale* **2019,** *11* (18), 9023-9031.
33. Tezgel, A. Ö.; Gonzalez-Perez, G.; Telfer, J. C.; Osborne, B. A.; Minter, L. M.; Tew, G. N., Novel Protein Transduction Domain Mimics as Nonviral Delivery Vectors for siRNA Targeting NOTCH1 in Primary Human T cells. *Molecular Therapy* **2013,** *21* (1), 201-209.
34. McKinlay, C. J.; Benner, N. L.; Haabeth, O. A.; Waymouth, R. M.; Wender, P. A., Enhanced mRNA delivery into lymphocytes enabled by lipid-varied libraries of charge-altering releasable transporters. *Proceedings of the National Academy of Sciences* **2018,** *115* (26), E5859-E5866.

35. Xie, Y.; Kim, N. H.; Nadithe, V.; Schalk, D.; Thakur, A.; Kılıç, A.; Lum, L. G.; Bassett, D. J. P.; Merkel, O. M., Targeted delivery of siRNA to activated T cells via transferrin-polyethylenimine (Tf-PEI) as a potential therapy of asthma. *Journal of Controlled Release* **2016,** *229*, 120-129.
36. Ding, Q.; Si, X.; Liu, D.; Peng, J.; Tang, H.; Sun, W.; Rui, M.; Chen, Q.; Wu, L.; Xu, Y., Targeting and liposomal drug delivery to CD40L expressing T cells for treatment of autoimmune diseases. *Journal of Controlled Release* **2015,** *207*, 86-92.
37. Patel, S.; Ashwanikumar, N.; Robinson, E.; DuRoss, A.; Sun, C.; Murphy-Benenato, K. E.; Mihai, C.; Almarsson, Ö.; Sahay, G., Boosting Intracellular Delivery of Lipid Nanoparticle-Encapsulated mRNA. *Nano Letters* **2017,** *17* (9), 5711-5718.
38. Arcaro, A.; Wymann, M. P., Wortmannin is a potent phosphatidylinositol 3-kinase inhibitor: the role of phosphatidylinositol 3,4,5-trisphosphate in neutrophil responses. *Biochemical Journal* **1993,** *296* (2), 297-301.
39. Tao, W.; Mao, X.; Davide, J. P.; Ng, B.; Cai, M.; Burke, P. A.; Sachs, A. B.; Sepp-Lorenzino, L., Mechanistically Probing Lipid-siRNA Nanoparticle-associated Toxicities Identifies Jak Inhibitors Effective in Mitigating Multifaceted Toxic Responses. *Molecular Therapy* **2011,** *19* (3), 567-575.
40. Vercauteren, D.; Piest, M.; van der Aa, L. J.; Al Soraj, M.; Jones, A. T.; Engbersen, J. F. J.; De Smedt, S. C.; Braeckmans, K., Flotillin-dependent endocytosis and a phagocytosis-like mechanism for cellular internalization of disulfide-based poly(amido amine)/DNA polyplexes. *Biomaterials* **2011,** *32* (11), 3072-3084.
41. von Kleist, L.; Stahlschmidt, W.; Bulut, H.; Gromova, K.; Puchkov, D.; Robertson, Mark J.; MacGregor, Kylie A.; Tomilin, N.; Pechstein, A.; Chau, N.; Chircop, M.; Sakoff, J.; von Kries, Jens P.; Saenger, W.; Kräusslich, H.-G.; Shupliakov, O.; Robinson, Phillip J.; McCluskey, A.; Haucke, V., Role of the Clathrin Terminal Domain in Regulating Coated Pit Dynamics Revealed by Small Molecule Inhibition. *Cell* **2011,** *146* (3), 471-484.
42. Macia, E.; Ehrlich, M.; Massol, R.; Boucrot, E.; Brunner, C.; Kirchhausen, T., Dynasore, a Cell-Permeable Inhibitor of Dynamin. *Developmental Cell* **2006,** *10* (6), 839-850.
43. Preta, G.; Cronin, J. G.; Sheldon, I. M., Dynasore - not just a dynamin inhibitor. *Cell Communication and Signaling* **2015,** *13* (1), 24.
44. Vercauteren, D.; Vandenbroucke, R. E.; Jones, A. T.; Rejman, J.; Demeester, J.; De Smedt, S. C.; Sanders, N. N.; Braeckmans, K., The Use of Inhibitors to Study Endocytic Pathways of Gene Carriers: Optimization and Pitfalls. *Molecular Therapy* **2010,** *18* (3), 561-569.
45. Rejman, J.; Bragonzi, A.; Conese, M., Role of clathrin- and caveolae-mediated endocytosis in gene transfer mediated by lipo- and polyplexes. *Molecular Therapy* **2005,** *12* (3), 468-474.
46. Rodal, S. K.; Skretting, G.; Garred, Ø.; Vilhardt, F.; van Deurs, B.; Sandvig, K., Extraction of Cholesterol with Methyl-β-Cyclodextrin Perturbs Formation of Clathrin-coated Endocytic Vesicles. *Molecular Biology of the Cell* **1999,** *10* (4), 961-974.
47. Novakowski, S.; Jiang, K.; Prakash, G.; Kastrup, C., Delivery of mRNA to platelets using lipid nanoparticles. *Scientific Reports* **2019,** *9* (1), 552.
48. Sahay, G.; Querbes, W.; Alabi, C.; Eltoukhy, A.; Sarkar, S.; Zurenko, C.; Karagiannis, E.; Love, K.; Chen, D.; Zoncu, R.; Buganim, Y.; Schroeder, A.; Langer, R.; Anderson, D. G., Efficiency of siRNA delivery by lipid nanoparticles is limited by endocytic recycling. *Nature Biotechnology* **2013,** *31* (7), 653-658.
49. Hajj, K. A.; Whitehead, K. A., Tools for translation: non-viral materials for therapeutic mRNA delivery. *Nature Reviews Materials* **2017,** *2* (10), 17056.
50. Miller, J. B.; Zhang, S.; Kos, P.; Xiong, H.; Zhou, K.; Perelman, S. S.; Zhu, H.; Siegwart, D. J., Non-Viral CRISPR/Cas Gene Editing In Vitro and In Vivo Enabled by Synthetic Nanoparticle Co-Delivery of Cas9 mRNA and sgRNA. *Angewandte Chemie International Edition* **2017,** *56* (4), 1059-1063.
51. Krohn-Grimberghe, M.; Mitchell, M. J.; Schloss, M. J.; Khan, O. F.; Courties, G.; Guimaraes, P. P.

G.; Rohde, D.; Cremer, S.; Kowalski, P. S.; Sun, Y.; Tan, M.; Webster, J.; Wang, K.; Iwamoto, Y.; Schmidt, S. P.; Wojtkiewicz, G. R.; Nayar, R.; Frodermann, V.; Hulsmans, M.; Chung, A.; Hoyer, F. F.; Swirski, F. K.; Langer, R.; Anderson, D. G.; Nahrendorf, M., Nanoparticle-encapsulated siRNAs for gene silencing in the haematopoietic stem-cell niche. *Nature Biomedical Engineering* **2020,** *4* (11), 1076-1089.

52. Dong, Y.; Love, K. T.; Dorkin, J. R.; Sirirungruang, S.; Zhang, Y.; Chen, D.; Bogorad, R. L.; Yin, H.; Chen, Y.; Vegas, A. J.; Alabi, C. A.; Sahay, G.; Olejnik, K. T.; Wang, W.; Schroeder, A.; Lytton-Jean, A. K. R.; Siegwart, D. J.; Akinc, A.; Barnes, C.; Barros, S. A.; Carioto, M.; Fitzgerald, K.; Hettinger, J.; Kumar, V.; Novobrantseva, T. I.; Qin, J.; Querbes, W.; Koteliansky, V.; Langer, R.; Anderson, D. G., Lipopeptide nanoparticles for potent and selective siRNA delivery in rodents and nonhuman primates. *Proceedings of the National Academy of Sciences* **2014,** *111* (11), 3955-3960.

53. Sago, C. D.; Lokugamage, M. P.; Paunovska, K.; Vanover, D. A.; Monaco, C. M.; Shah, N. N.; Gamboa Castro, M.; Anderson, S. E.; Rudoltz, T. G.; Lando, G. N.; Munnilal Tiwari, P.; Kirschman, J. L.; Willett, N.; Jang, Y. C.; Santangelo, P. J.; Bryksin, A. V.; Dahlman, J. E., High-throughput in vivo screen of functional mRNA delivery identifies nanoparticles for endothelial cell gene editing. *Proceedings of the National Academy of Sciences* **2018,** *115* (42), E9944-E9952.

54. Ball, R. L.; Hajj, K. A.; Vizelman, J.; Bajaj, P.; Whitehead, K. A., Lipid Nanoparticle Formulations for Enhanced Co-delivery of siRNA and mRNA. *Nano Letters* **2018,** *18* (6), 3814-3822.

55. Van Rossenberg, S. M.; Sliedregt-Bol, K. M.; Meeuwenoord, N. J.; Van Berkel, T. J.; Van Boom, J. H.; Van Der Marel, G. A.; Biessen, E. A., Targeted lysosome disruptive elements for improvement of parenchymal liver cell-specific gene delivery. *Journal of Biological Chemistry* **2002,** *277* (48), 45803-45810.

56. de Bruin, K. G.; Fella, C.; Ogris, M.; Wagner, E.; Ruthardt, N.; Bräuchle, C., Dynamics of photoinduced endosomal release of polyplexes. *Journal of Controlled Release* **2008,** *130* (2), 175-182.

57. Selbo, P. K.; Weyergang, A.; Høgset, A.; Norum, O.-J.; Berstad, M. B.; Vikdal, M.; Berg, K., Photochemical internalization provides time- and space-controlled endolysosomal escape of therapeutic molecules. *Journal of Controlled Release* **2010,** *148* (1), 2-12.

58. Tai, W.; Gao, X., Functional peptides for siRNA delivery. *Advanced Drug Delivery Reviews* **2017,** *110-111*, 157-168.

59. Saar, K.; Lindgren, M.; Hansen, M.; Eiríksdóttir, E.; Jiang, Y.; Rosenthal-Aizman, K.; Sassian, M.; Langel, Ü., Cell-penetrating peptides: A comparative membrane toxicity study. *Analytical Biochemistry* **2005,** *345* (1), 55-65.

60. Martens, T. F.; Remaut, K.; Demeester, J.; De Smedt, S. C.; Braeckmans, K., Intracellular delivery of nanomaterials: How to catch endosomal escape in the act. *Nano Today* **2014,** *9* (3), 344-364.

61. Sahin, U.; Karikó, K.; Türeci, Ö., mRNA-based therapeutics — developing a new class of drugs. *Nature Reviews Drug Discovery* **2014,** *13* (10), 759-780.

62. Foster, J. B.; Barrett, D. M.; Karikó, K., The Emerging Role of In Vitro-Transcribed mRNA in Adoptive T Cell Immunotherapy. *Molecular Therapy* **2019,** *27* (4), 747-756.

63. Rosenberg, S. A.; Restifo, N. P., Adoptive cell transfer as personalized immunotherapy for human cancer. *Science* **2015,** *348* (6230), 62-68.

64. DiTommaso, T.; Cole, J. M.; Cassereau, L.; Buggé, J. A.; Hanson, J. L. S.; Bridgen, D. T.; Stokes, B. D.; Loughhead, S. M.; Beutel, B. A.; Gilbert, J. B.; Nussbaum, K.; Sorrentino, A.; Toggweiler, J.; Schmidt, T.; Gyuelveszi, G.; Bernstein, H.; Sharei, A., Cell engineering with microfluidic squeezing preserves functionality of primary immune cells in vivo. *Proceedings of the National Academy of Sciences* **2018,** *115* (46), E10907-E10914.

65. Roth, T. L.; Puig-Saus, C.; Yu, R.; Shifrut, E.; Carnevale, J.; Li, P. J.; Hiatt, J.; Saco, J.; Krystofinski, P.; Li, H.; Tobin, V.; Nguyen, D. N.; Lee, M. R.; Putnam, A. L.; Ferris, A. L.; Chen, J.

W.; Schickel, J.-N.; Pellerin, L.; Carmody, D.; Alkorta-Aranburu, G.; del Gaudio, D.; Matsumoto, H.; Morell, M.; Mao, Y.; Cho, M.; Quadros, R. M.; Gurumurthy, C. B.; Smith, B.; Haugwitz, M.; Hughes, S. H.; Weissman, J. S.; Schumann, K.; Esensten, J. H.; May, A. P.; Ashworth, A.; Kupfer, G. M.; Greeley, S. A. W.; Bacchetta, R.; Meffre, E.; Roncarolo, M. G.; Romberg, N.; Herold, K. C.; Ribas, A.; Leonetti, M. D.; Marson, A., Reprogramming human T cell function and specificity with non-viral genome targeting. *Nature* **2018,** *559* (7714), 405-409.

66. Wang, X.; Rivière, I., Clinical manufacturing of CAR T cells: foundation of a promising therapy. *Molecular Therapy - Oncolytics* **2016,** *3*, 16015.

67. Pardi, N.; Hogan, M. J.; Porter, F. W.; Weissman, D., mRNA vaccines — a new era in vaccinology. *Nature Reviews Drug Discovery* **2018,** *17* (4), 261-279.

68. Finn, J. D.; Smith, A. R.; Patel, M. C.; Shaw, L.; Youniss, M. R.; van Heteren, J.; Dirstine, T.; Ciullo, C.; Lescarbeau, R.; Seitzer, J.; Shah, R. R.; Shah, A.; Ling, D.; Growe, J.; Pink, M.; Rohde, E.; Wood, K. M.; Salomon, W. E.; Harrington, W. F.; Dombrowski, C.; Strapps, W. R.; Chang, Y.; Morrissey, D. V., A Single Administration of CRISPR/Cas9 Lipid Nanoparticles Achieves Robust and Persistent In Vivo Genome Editing. *Cell Reports* **2018,** *22* (9), 2227-2235.

69. Liu, J.; Chang, J.; Jiang, Y.; Meng, X.; Sun, T.; Mao, L.; Xu, Q.; Wang, M., Fast and Efficient CRISPR/Cas9 Genome Editing In Vivo Enabled by Bioreducible Lipid and Messenger RNA Nanoparticles. *Advanced Materials* **2019,** *31* (33), 1902575.

70. Anzalone, A. V.; Randolph, P. B.; Davis, J. R.; Sousa, A. A.; Koblan, L. W.; Levy, J. M.; Chen, P. J.; Wilson, C.; Newby, G. A.; Raguram, A.; Liu, D. R., Search-and-replace genome editing without double-strand breaks or donor DNA. *Nature* **2019,** *576* (7785), 149-157.

Supporting Information

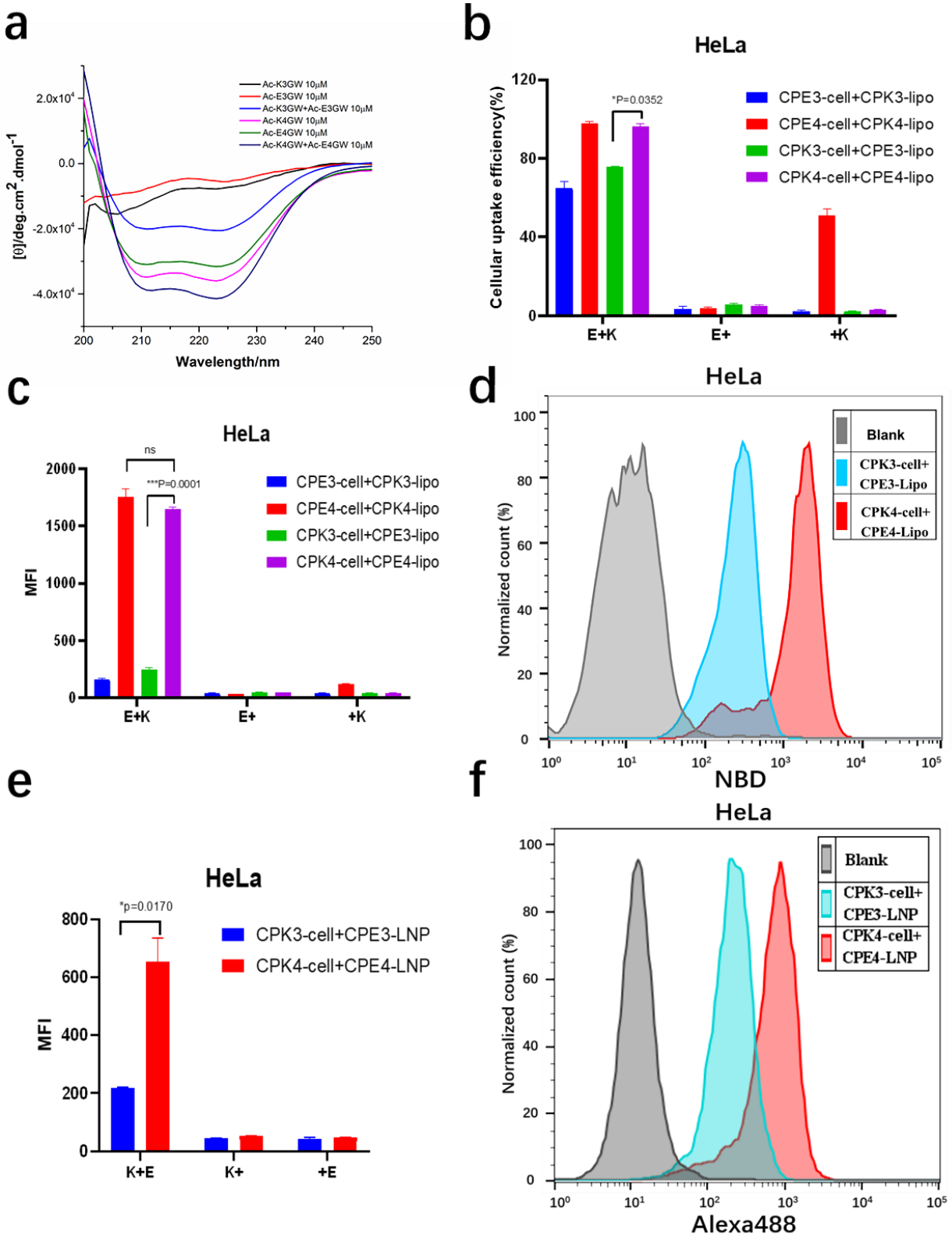

SI Figure 1. Evaluation of coiled-coil peptide pair mediated uptake in liposomes and LNPs. (a) CD spectra of K3/E3 and K4/E4 pairs. Peptides were dissolved at a total concentration of 10 μM in PBS at pH 7.4, and spectra

were measured at 20℃. **(b)** Cellular uptake of liposomes in HeLa cells. Uptake efficiency was calculated by quantifying the NBD-positive cells. **(c-d)** The fluorescence intensity (MFI) of cellular internalization of liposomes with HeLa cells. Lipid compositions of liposomes: DOPC/DOPE/cholesterol=2:1:1, 1 mol% of the NBD-PE served as the fluorescent dye, 1 mol% of the CPK (3 or 4) or CPE (3 or 4) were added for lipopeptide modified liposomes. E+K: both E and K peptide included; E+: only E peptide included; K+: only K peptide included. **(e-f)** The fluorescence intensity of cellular internalization of LNPs encapsulated nucleic acid by CPE3/4-LNP with HeLa cells pretreated with CPK3/4. Alexa488 labeled nucleic acid was encapsulated and served as the fluorescent dye. Unpaired t-test was used to determine the significance of the comparisons of data indicated in **b**, **c**, and **d** (*P < 0.05; **P < 0.01; ***P < 0.001; ****P < 0.0001). In all panels, error bars represent mean ± s.d. (n=3).

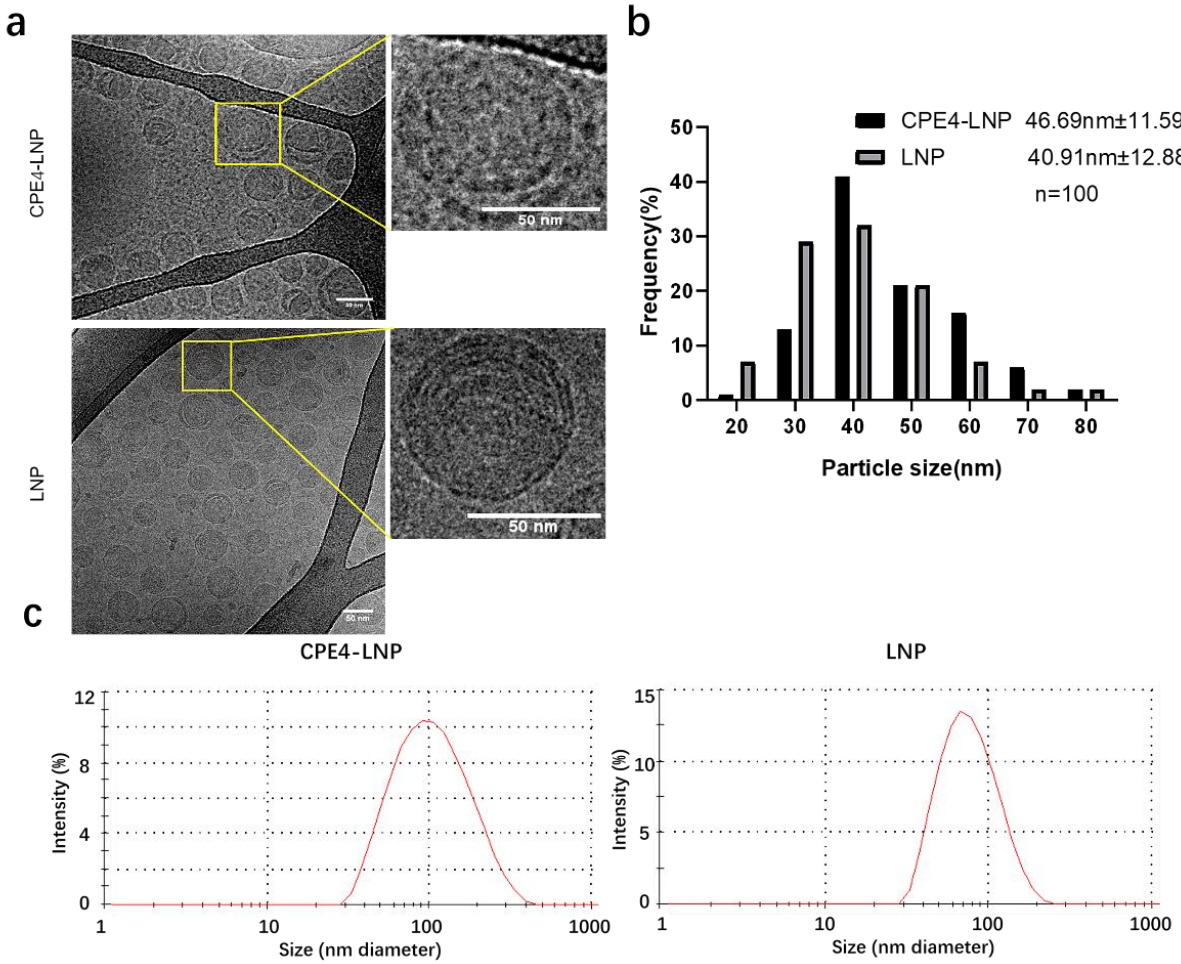

SI Figure 2 (a) Cryo-EM images of Alexa488-nucleic acid encapsulated CPE4-LNP and LNP. **(b)** Size distribution of Alexa488-nucleic acid encapsulated LNPs as determined by cryo-EM. The values derived from the frequency distribution graphs represent mean ± s.d. (n=100). Scale bar is 50 nm. **(c)** Size distribution of Alexa488-nucleic acid encapsulated LNPs according to DLS.

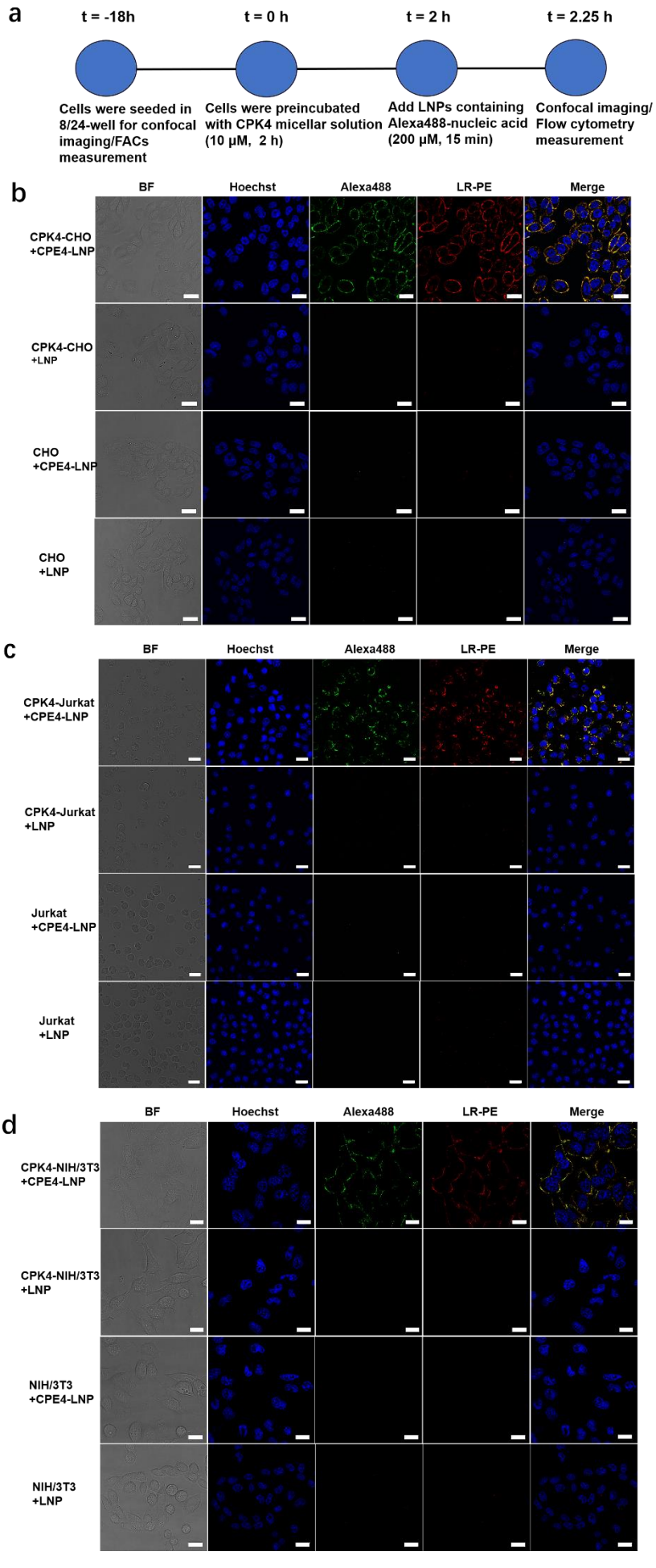
a
t = -18h
t = 0 h
t = 2 h
t = 2.25 h
Cells were seeded in 8/24-well for confocal imaging/FACs measurement
Cells were preincubated with CPK4 micellar solution (10 μM, 2 h)
Add LNPs containing Alexa488-nucleic acid (200 μM, 15 min)
Confocal imaging/ Flow cytometry measurement
b
BF
Hoechst
Alexa488
LR-PE
Merge
CPK4-CHO +CPE4-LNP
CPK4-CHO +LNP
CHO +CPE4-LNP
CHO +LNP
c
BF
Hoechst
Alexa488
LR-PE
Merge
CPK4-Jurkat +CPE4-LNP
CPK4-Jurkat +LNP
Jurkat +CPE4-LNP
Jurkat +LNP
d
BF
Hoechst
Alexa488
LR-PE
Merge
CPK4-NIH/3T3 +CPE4-LNP
CPK4-NIH/3T3 +LNP
NIH/3T3 +CPE4-LNP
NIH/3T3 +LNP

SI Figure 3. (a) Schematic representation of the LNPs uptake experiments with cells. **(b)** Confocal microscopic images of LNPs uptake with CHO cells. **(c)** with NIH/3T3 cells. **(d)** with Jurkat cells. Cells were preincubated with a micellar CPK4 solution (10 μM, 200 μL, 2 h). After removal of the medium, the LNPs containing Alexa488-nucleic acid were added (200 μM, 200 μL, 15 min), then cells were washed before imaging. Blue: Hoechst 33342; green: Alexa488-nucleic acid; red: LR-PE; BF: bright field. Scale bar is 20 μm.

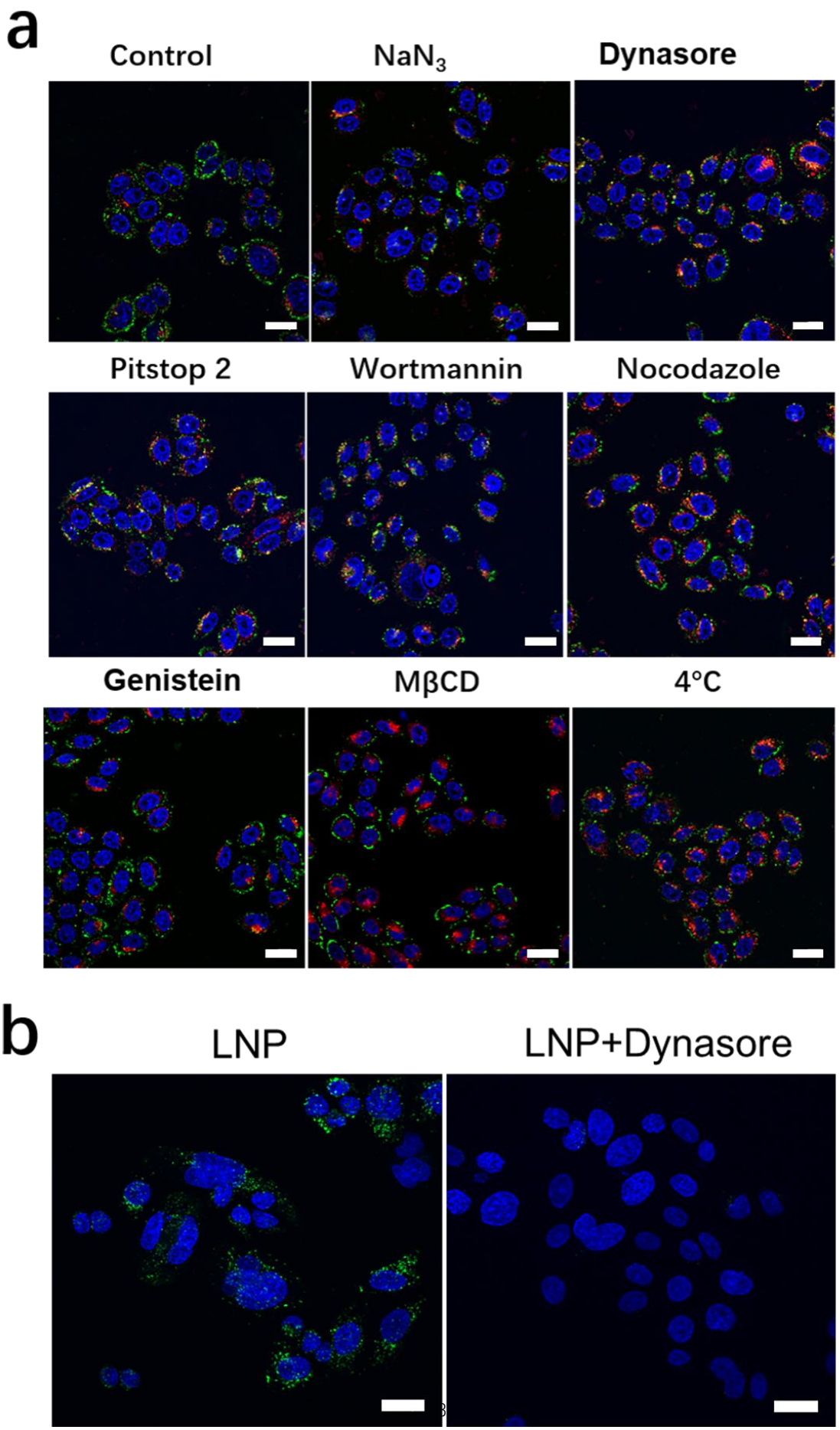
a
Control
NaN3
Dynasore
Pitstop 2
Wortmannin
Nocodazole
Genistein
MβCD
4°C
b
LNP
LNP+Dynasore

SI Figure 4. (a) Confocal microscopic images of cellular uptake of CPE4-LNP with CPK4-HeLa cells in the presence of endocytosis inhibitors. HeLa cells were first treated with different endocytosis inhibitors (1 h), followed by lyso-tracker deep red (75 nM, 200 μL) and CPK4 (10 μM, 200 μL, 2 h, in the presence of fresh inhibitors) incubation, then CPE4-LNP (200 μM, 200 μL, 15 min) were added together with fresh inhibitors, then cells were washed and added with phenol red free DMEM before imaging. Blue: Hoechst 33342; green: Alexa488-nucleic acid; red: lyso-tracker deep red. **(b)** Confocal microscopic images of cellular internalization of LNP with HeLa cells with endocytosis inhibitor dynasore. HeLa cells were pretreated with dynasore (80 μM, 200 μL, 1 h), then LNP (200 μM, 200 μL, 4 h) were incubated with the presence of fresh dynasore, and cells were washed before imaging. Blue: Hoechst 33342; green: Alexa488-nucleic acid. Scale bar is 20 μm.

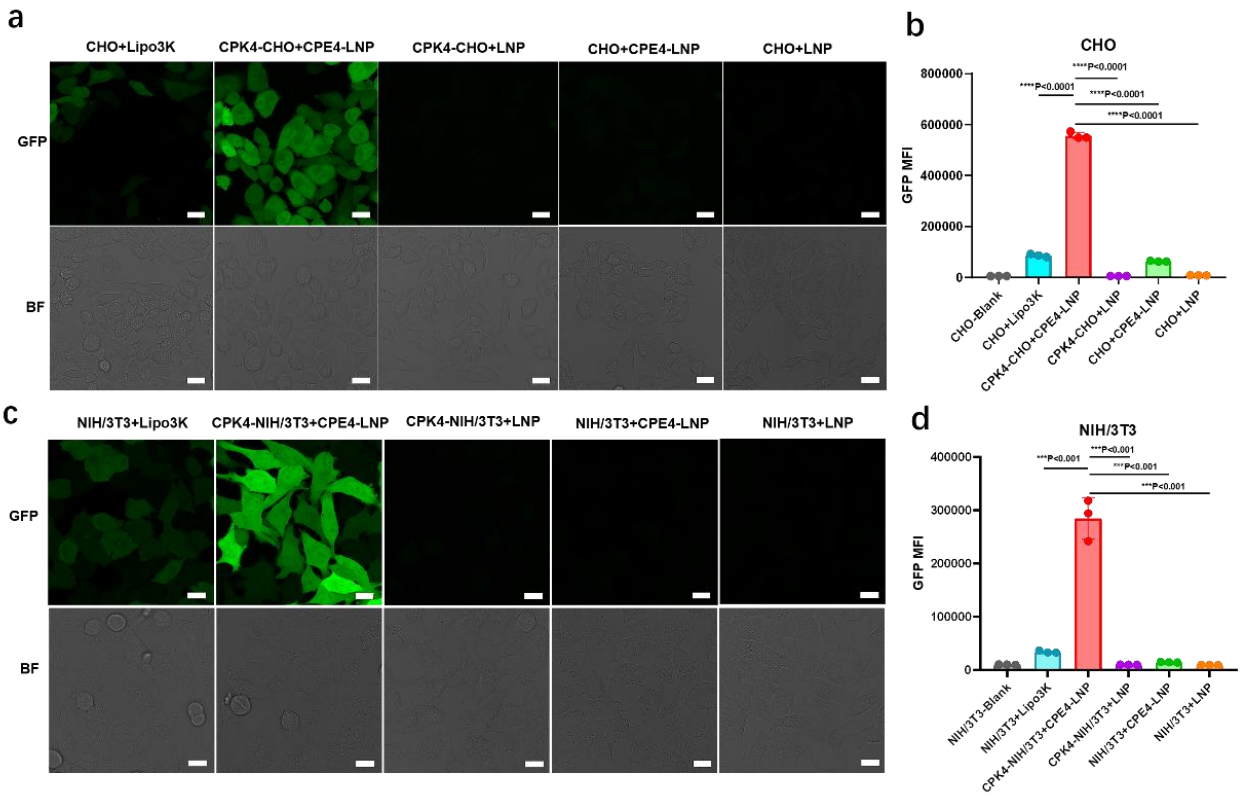

SI Figure 5 (a) Confocal microscopic images of the EGFP-mRNA transfection of LNPs with CHO cells. Scale bar is 20 μm. **(b)** The GFP expression fluorescence intensity (GFP MFI) of LNPs with CHO cells. **(c)** Confocal microscopic images of the EGFP-mRNA transfection of LNPs with NIH/3T3 cells. Scale bar is 20 μm. **(d)** The GFP expression fluorescence intensity (GFP MFI) of LNPs with NIH/3T3 cells. Cells were pretreated with CPK4 solution (10 μM, 200 μL, 2 h), after removal of the medium, EGFP-mRNA encapsulated LNPs were added (1 μg/mL, 200 μL, 2 h), and then cultured for another 18-24 h before imaging and flow cytometry measurements. Lipo3K: lipofectamine 3K; GFP: green fluorescent protein; BF: bright field. Unpaired student t-test was used to determine the significance of the comparisons of data indicated in **b**, and **d** (*P < 0.05; **P < 0.01; ***P < 0.001; ****P < 0.0001). In all panels, error bars represent mean ± s.d. (n=3).

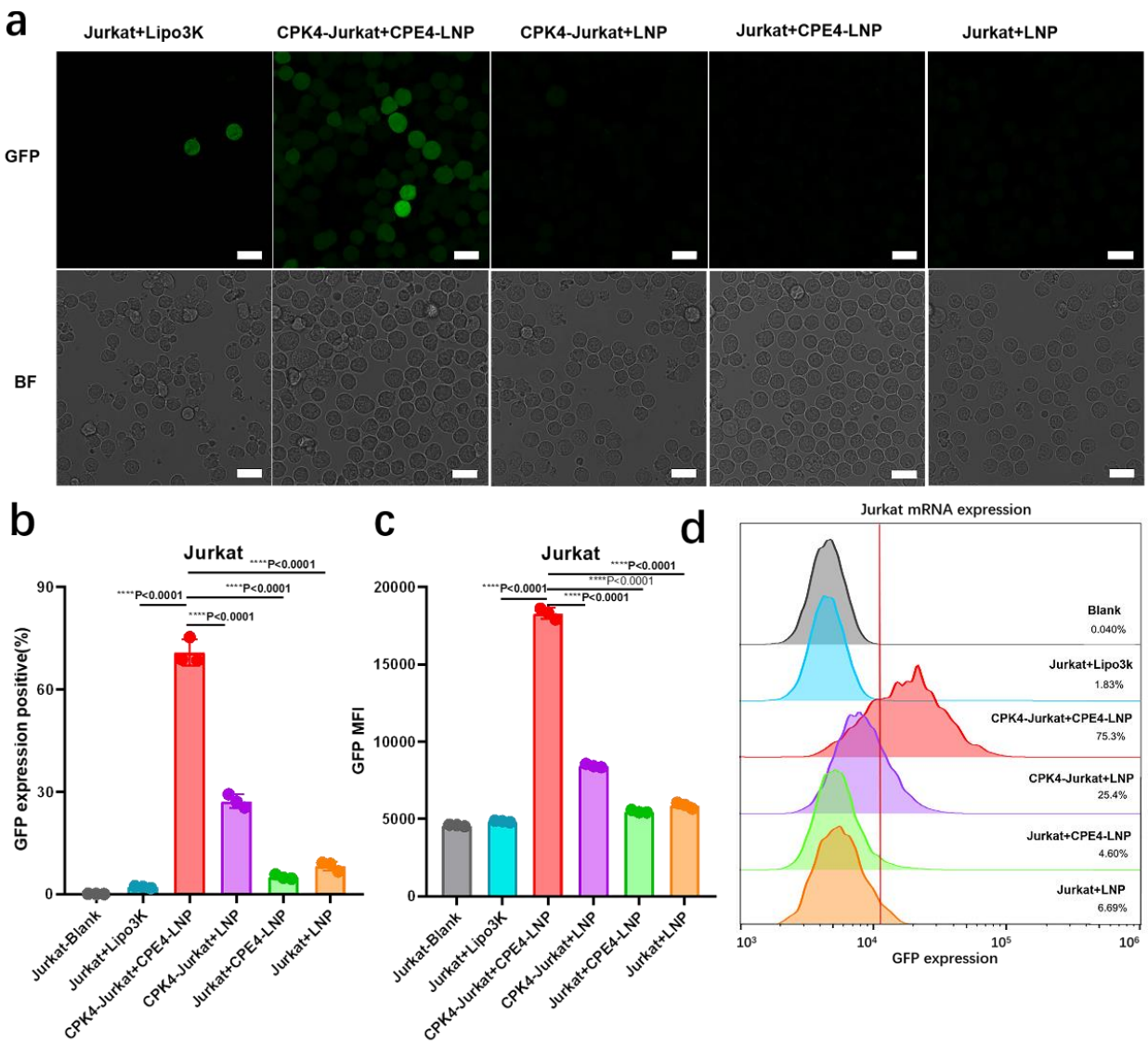

SI Figure 6. Transfection efficiency of the fusogenic coiled-coil peptide system with Jurkat cells. (a) Confocal microscopic images of the EGFP-mRNA transfection of LNPs. Lipo3K: lipofectamine 3K; GFP: green fluorescent protein; BF: bright field. Scale bar is 20 μm. **(b)** The quantification of EGFP-mRNA transfection efficiency of LNPs. **(c-d)** The GFP expression fluorescence intensity (GFP MFI) of LNPs. Jurkat cells were first incubated with CPK4 (10 μM, 200 μL, 2 h), followed by EGFP-mRNA encapsulated LNPs were incubated (1 μg/mL, 200 μL, 2 h), after that, cells were washed 3 times and cultured for another 18-24h before imaging and flow cytometry measurements. Unpaired student t-test was used to determine the significance of the comparisons of data indicated in **b**, and **c** (*P < 0.05; **P < 0.01; ***P < 0.001; ****P < 0.0001). In all panels, error bars represent mean ± s.d. (n=3).

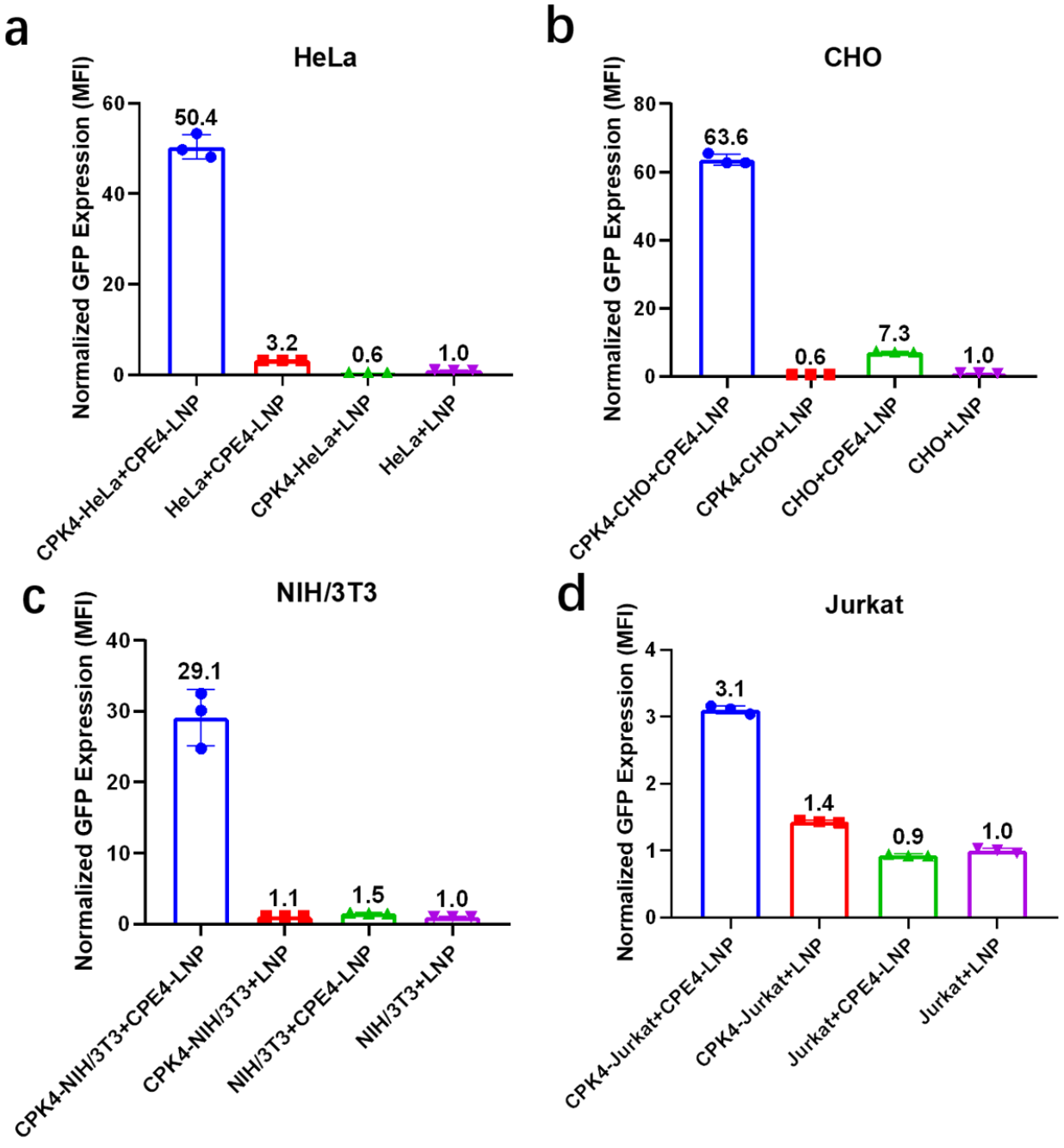

SI Figure 7. GFP fluorescence enhancement. The protein expression fold number of GFP fluorescence intensity (GFP MFI) of groups normalized to plain LNP **(a)** with HeLa cells, (**b)** with CHO cells, (**c)** with NIH/3T3 cells, (**d)** with Jurkat cells. In all panels, error bars represent mean ± s.d. (n=3).

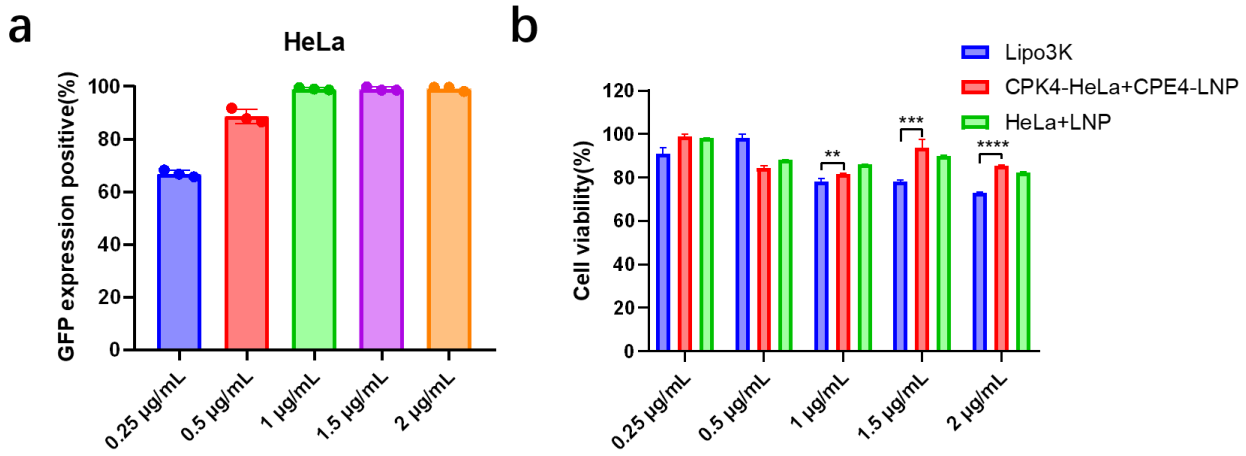

SI Figure 8 (a) Transfection efficiency of different concentrations of EGFP-mRNA encapsulated CPE4-LNP with HeLa cells pretreated with CPK4. HeLa cells were first incubated with CPK4 (10 μM, 200 μL, 2 h), followed by different concentrations of EGFP-mRNA encapsulated CPE4-LNP incubation (2 h), then the medium was removed, cells were washed and cultured for another 18-24 h before flow cytometry measurements. **(b)** The cell viability evaluation of EGFP-mRNA encapsulated LNPs after transfection. HeLa cells were first incubated with CPK4 (10 μM, 200 μL, 2 h), followed by different concentrations of EGFP-mRNA encapsulated LNPs incubation (2 h), then the medium was removed, and cells were washed and cultured for another 24 h. After that, WST-1 solution (20 μL) was added to the medium (200 μL) and incubated for 4 h before measuring. Unpaired student t-test was used to determine the significance of the comparisons of data indicated in **b** (*P < 0.05; **P < 0.01; ***P < 0.001; ****P < 0.0001). In all panels, error bars represent mean ± s.d. (n=3).